



Concepts for the Future Exploration of Dwarf Planet Ceres' Habitability

Julie Castillo-Rogez¹, John Brophy¹, Kelly Miller², Michael Sori³, Jennifer Scully¹, Lynnae Quick⁴, Robert Grimm⁵, Michael Zolensky⁶, Michael Bland⁷, Debra Buczkowski⁸, Carol Raymond¹, Amanda Hendrix⁹, Thomas Prettyman⁹, Yasuhito Sekine¹⁰, Timothy Titus⁷, David Williams¹¹, Paul Backes¹, Laura Barge¹, Anton Ermakov¹², Andrew Galassi¹, Scott Moreland¹, and Kris Zacny¹³

¹ Jet Propulsion Laboratory, California Institute of Technology, 4800 Oak Grove Drive, Pasadena CA, 91109, USA; Julie.C.Castillo@jpl.nasa.gov

² Southwest Research Institute, 6220 Culebra Road, San Antonio, TX 78238, USA

³ Purdue University, 610 Purdue Mall, West Lafayette, IN 47907, USA

⁴ Goddard Space Flight Center, 8800 Greenbelt Road, Greenbelt, MD 20771, USA

⁵ Southwest Research Institute Boulder Office, 1050 Walnut Street, Suite 300, Boulder, CO 80302, USA

⁶ Johnson Space Center, NASA, 2101 E NASA Parkway, Houston, TX 77058, USA

⁷ United States Geological Survey, Astrogeology Science Center, Flagstaff, AZ 86001, USA

⁸ Johns Hopkins University, Applied Physics Laboratory, 11100 Johns Hopkins Road, Laurel, MD 20723, USA

⁹ Planetary Science Institute, 1700 E Fort Lowell Road, Ste 106, Tucson, AZ 85719, USA

¹⁰ Earth-Life Science Institute, Tokyo Institute of Technology, 1 Chome-31 Ishikawacho, Ota City, Tokyo 145-0061, Japan

¹¹ Arizona State University, School of Earth and Space Exploration, 781 Terrace Mall, Tempe, AZ 85287, USA

¹² University of California Berkeley, Berkeley, CA 94720, USA

¹³ Honeybee Robotics, 2408 Lincoln Avenue, Altadena, CA 91001, USA

Received 2020 November 25; revised 2021 August 23; accepted 2021 October 20; published 2022 February 18

Abstract

Dwarf planet Ceres is a compelling target for future exploration because it hosts at least regional brine reservoirs and potentially ongoing geological activity. As the most water-rich body in the inner solar system, it is a representative of a population of planetesimals that were likely a significant source of volatiles and organics to the inner solar system. Here we describe possible medium-class (around \$1 billion) mission concepts that would determine both Ceres' origin and its current habitability potential. Habitability is addressed through a combination of geological, geophysical, and compositional investigations by (i) searching for evidence from orbit of past and ongoing geological activity near landforms interpreted as brine-driven volcanic structures and (ii) probing the brine distribution below one of these regions with electromagnetic sounding (in situ). Two approaches were considered for compositional measurements, which address both habitability and origins: (1) in situ exploration at two sites and (2) sample return from a single site. Both concepts targeted material at Occator crater, which is one of the youngest features on Ceres (~20 Ma) and a site rich in evaporites evolved from recently erupted brine sourced from a region >35 km deep. We conclude that a sample return architecture from these young evaporite deposits offers greater science return by enabling high-resolution analysis of organic matter (trapped in salt minerals) and isotopes of refractory elements for a similar cost and less science risk than in situ analyses. This manuscript describes the six science objectives and the two implementation concepts considered to achieve those objectives.

Unified Astronomy Thesaurus concepts: [Ceres \(219\)](#); [Cosmochemistry \(331\)](#); [Landers \(901\)](#)

1. Science Definition

1.1. Science Motivations for Ceres' Exploration

Dwarf planet Ceres is the largest object in the main belt and the most water-rich (~25 wt.%) object in the inner solar system (in relative abundance). Ceres had sufficient water and radioisotope-bearing silicates to host a deep ocean in its past, leading to a layered interior structure with a high degree of aqueous alteration (Ermakov et al. 2017). The Dawn mission revealed evidence of recent and possibly ongoing geologic activity on Ceres (De Sanctis et al. 2020), the presence of liquid below an ice-rich crust (Fu et al. 2017; Scully et al. 2020), local surface deposits of organic matter (De Sanctis et al. 2017), potentially superchondritic concentrations of carbon in the regolith (Prettyman et al. 2018), and the presence of an exosphere and volatile transport (Raponi et al. 2018). Recent brine-driven exposure of material onto Ceres' surface can be found at Occator crater (<2 Ma; Nathues et al. 2020)

and the ~4 km tall, geologically recent Ahuna Mons (<100 Ma; Ruesch et al. 2016, 2019a). Multiple lines of evidence for deep liquid, at least regionally, and long-lived heat sources qualify Ceres as an ocean world (Castillo-Rogez et al. 2020) per the Hendrix et al. (2019) definition, even if Ceres is undergoing advanced freezing. A detailed evaluation of Ceres' habitability potential can be found in the review by Castillo-Rogez (2020), which forms the basis for the assessment of the state of knowledge of Ceres against the Roadmap to Ocean Worlds (ROW; Figure 1). These observations suggest that Ceres is a prime destination to study habitability on icy worlds. An independent origin of life in Ceres is unlikely based on the dwarf planet's limited heat budget (Castillo-Rogez 2020). However, investigation of Ceres would provide a critical data point for understanding how ocean worlds work (by separating the tidal heating variable) to maintain habitability through billions of years. Furthermore, Ceres offers context for understanding how volatiles and organic compounds were generated and transported throughout the solar system, and it may represent planetesimals that were the source of (some of) Earth's volatiles (Budde et al. 2019). These scientific motivations are the drivers for this concept of a Ceres in situ and sample return explorer.



Original content from this work may be used under the terms of the [Creative Commons Attribution 4.0 licence](#). Any further distribution of this work must maintain attribution to the author(s) and the title of the work, journal citation and DOI.

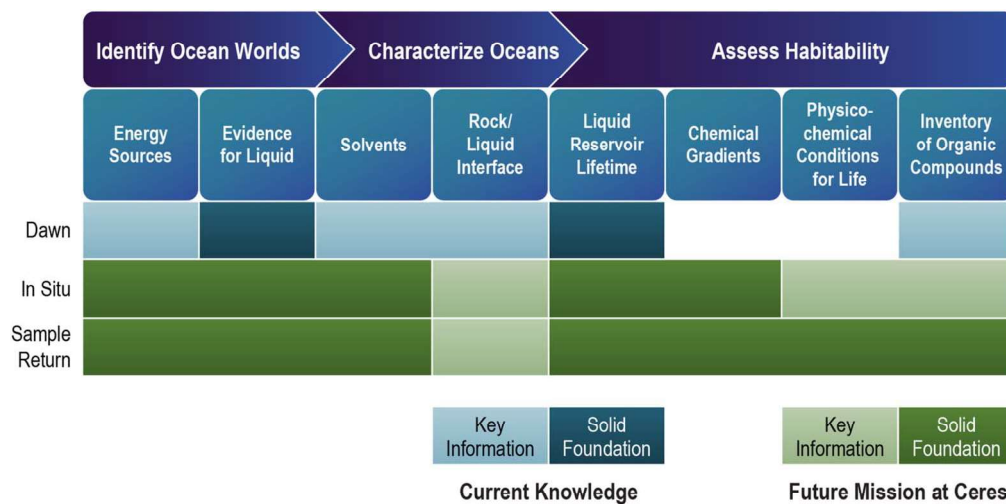


Figure 1. Knowledge of Ceres' astrobiological potential framed in the context of the ROW based on Dawn's results. "Solid foundation" refers to direct observational constraints, while "key information" refers to indirect observational inferences and theoretical models. A future in situ mission or sample return would significantly progress along the roadmap. (Adapted from Hendrix et al. 2019 and based on an analysis by Castillo-Rogez 2020.)

1.2. Science Questions and Objectives

The overarching goals of this concept are to (1) assess Ceres' current habitability and use Ceres as a test case for determining the habitability of volatile-rich bodies over time and (2) determine Ceres' origin and the relationship of its volatiles and organics to other inner solar system bodies. Goal 1 is addressed via objectives 1–5, whereas goal 2 is addressed via objective 6.

1.2.1. Objective 1: Test whether Extrusion from a Brine-rich Mantle Occurred during Ceres' Recent History

Assessing Ceres' habitability through time requires understanding the mechanisms of material exchange between the interior and the surface. Evidence for intrusion of deep mantle material into the shallow subsurface has been found in association with features likely of cryovolcanic origin, including Ahuna Mons (Ruesch et al. 2019a), the Occator faculae (Cerealia Facula, Pasola Facula, and Vinalia Faculae; Nathues et al. 2020; Scully et al. 2020), and, potentially, Haulani crater (A. Nathues 2021, personal communication). Ceres' numerous mounds and domes (e.g., Cosecha Tholus), which are observed across substantial portions of its surface, have also been attributed to cryovolcanism (Sori et al. 2017, 2018).

Such deeply sourced cryovolcanism provides a key mechanism for subsurface–surface exchange that might introduce chemical gradients in the crust over time and create transient habitable regions. However, alternative nonvolcanic processes have also been proposed for the formation of the many mounds and domes (Bland et al. 2019). The latter require a heterogeneous crust but potentially only limited exchange between the deep mantle and the shallow subsurface. Characterizing the lateral structure of Ceres' crust is necessary to resolve this ambiguity.

Spatial variations in composition and structure can be inferred from spatial variations in subsurface density. This would be investigated through the determination of local high-degree gravity in association with the domes ($n > 40$ versus $n = 18$ for the global Ceres gravity field from Dawn; Konopliv et al. 2018), as has been done for Ahuna Mons (Ruesch et al. 2019a). Medium-resolution (a few meters per pixel) color imaging can reveal structural features that inform on the emplacement mechanism, as recently published for the Occator faculae (e.g., Scully et al. 2020).

1.2.2. Objective 2: Test whether Endogenic Activity Is Ongoing at Occator Crater

Results from the Dawn second extended mission (XM2; see Castillo-Rogez & Rayman 2020) suggest very recent (< 2 Ma) and potentially ongoing activity at Cerealia Facula based on crater counting (Nathues et al. 2020) and the occurrence of hydrohalite ($\text{NaCl} \cdot 2\text{H}_2\text{O}$), which dehydrates within hundreds of years when exposed on Ceres' surface (De Sanctis et al. 2020). Ongoing activity at Vinalia Faculae is also suspected, but definitive evidence is lacking. Seeking additional evidence for brine exposure at Occator crater, in combination with objectives 1, 3, and 4 (brine depth and composition determination), would inform on the mechanism(s) driving recent and current activity.

Landscape modification since the Dawn observations (2015–2018) could be found from imaging the Occator faculae at a resolution similar to Dawn XM2 (< 5 m pixel $^{-1}$) and looking for changes in the distribution of bright material. At Cerealia Facula, material exposure is expected to occur at the top of Cerealia Tholus (De Sanctis et al. 2020), where the addition of evaporites may not be detectable against the bright background. On the other hand, material exposure at Vinalia Faculae, if ongoing, is expected to be a dominantly ballistic process, hence resulting in a relative increase of evaporites against the dark floor. Based on eruption rates from Quick et al. (2019), the predicted volume of material that may be exposed over a period of 20 yr at Vinalia Faculae may be equivalent to a surface area of 0.5–2 km 2 . If all of the predicted volume of material were exposed onto the dark floor, it would fill 2×10^4 – 8×10^4 pixels at 5 m pixel $^{-1}$. The uncertainty is due to limited knowledge of the fracture widths (from which the Vinalia Faculae–forming brines are proposed to originate) and the brine ascension rate. It is possible, especially for the lower end of that range, that freshly exposed material would not be detectable because it overlaps with previous exposures. As there are multiple sources of evaporites at Vinalia Faculae, it is reasonable to assume that some of the recently deposited material would occur in an area that did not contain evaporites at the time of the Dawn observations. Nevertheless, a nondetection at 5 m pixel $^{-1}$ resolution would set a bound on the extrusion rate.

Imaging at 5 m pixel $^{-1}$ enables the setting of the freshly exposed material to be analyzed and interpreted, which allows

Table 1
Range of Values for Habitability Parameters, Modified from Cockell et al. (2016)

Habitability Parameters	Range of Conditions Amenable to Life	Measurements by Future Mission
Temperature (T) and physico-chemical conditions	$T = -25^{\circ}\text{C}$ (limit for metabolic activity) to 122°C (limit for microbial growth) and up to 150°C (cell repair); water activity >0.605 ; redox between -1 and $+1.5$; no known limit on pH	Brine eutectic water activity, redox (Eh), temperature inferred from mineralogy and isotopes of volatiles, and phase relationships
Available energy	e.g., NH_3 , NH_4^+ , Fe(II) , Fe(III) , SO_2 , SO_4^{2-} .	Occurrence and concentration of electron donors and acceptors
Presence of major elements	Carbon, hydrogen, nitrogen, oxygen, phosphorus, sulfur (CHNOPS present), iron, and other metals	Inventory of elemental compounds and form (mineral, organics)

for secondary emplacement processes (e.g., mass wasting) to be differentiated from primary emplacement processes (e.g., the ballistic and/or short-lived flow emplacement of the endogenic material; e.g., Quick et al. 2019). For example, mass wasting is associated with specific topographic conditions (e.g., negative slope), while ballistic emplacement of endogenic materials results in characteristically diffuse deposits of bright material, such as those observed in Vinalia Faculae; these deposits are morphologically distinct from material emplaced via mass wasting, such as at the narrow bright landslides that cascade into the fractures associated with Vinalia Faculae (see Scully et al. 2021). Color imaging would further help identify freshly emplaced carbonates and chlorides (Bu et al. 2019; De Sanctis et al. 2020; Nathues et al. 2020) by comparisons with the Dawn data sets.

1.2.3. Objective 3: Determine the Depth of Liquid Water below Occator

Recent activity (<2 Ma) at Occator crater is interpreted to stem from a deeply sourced brine rich in carbonates and chlorides (Quick et al. 2019; Raymond et al. 2020; Figure 2). An origin solely from a chamber generated by the Occator-forming impact heat is uncertain because the lifetime of such a chamber predicted by thermal modeling (<5 Ma; Hesse & Castillo-Rogez 2019) is substantially less than the age of the crater (~ 20 Ma; Nathues et al. 2020). Furthermore, an impact melt chamber in the central region of Occator crater is tens of kilometers away from the Vinalia Faculae, too far to represent a viable source for those features (Scully et al. 2020). Medium-resolution gravity data returned during XM2 support the presence of a deep brine layer below Occator crater (Raymond et al. 2020), but its depth is poorly constrained. More precise knowledge of its depth and extent would provide a critical constraint on the thermal state of the crust and the drivers of activity at Ceres. For example, it has been suggested that a high fraction of gas and salt hydrates in the crust could slow down heat transfer by preventing convection onset (Formisano et al. 2020) and decreasing the crust thermal conductivity (Castillo-Rogez et al. 2019) and thus help maintain deep liquid until present. A similar explanation has been suggested for the long-term preservation of a deep ocean on Pluto (Kamata et al. 2019). More generally, knowledge of the temperature gradient in the crust would put the broad Dawn geological results in context.

Geophysical sounding is required to address this objective. Seismometry was initially considered but discarded due to surface coupling requirements and uncertainty in the seismic sources. Furthermore, unknown/ambiguous crustal material properties might limit the interpretation of seismic sounding. Electromagnetic sounding was identified as the optimal

approach for detecting brines because of the high inductive response of salty water and because the solar wind source has been characterized (see Grimm et al. 2020 for details).

1.2.4. Objective 4: Characterize Ceres' Deep Brine Environment at Occator Crater

The evaporites exposed in Occator crater sample the deep brine (Nathues et al. 2020; Scully et al. 2020) and offer a unique opportunity to investigate the brine environment of an ocean world nearing global freezing. Dawn revealed abundant sodium carbonate and smaller fractions of ammonium chlorides and hydrohalite (De Sanctis et al. 2016, 2020; Raponi et al. 2019). These indicate an alkaline source with a temperature above 245 K (Castillo-Rogez et al. 2018). The next natural step in the exploration of Ceres is to test whether the mud/brine is currently habitable via determination of attributes of the environment in which the brines formed, including temperature, pH, H_2 fugacity, chemical gradient (Table 1), and chemicals harmful to life. Some of these constraints exist for Ceres' early ocean environment from the mineralogical and elemental data from the Dawn mission (Castillo-Rogez et al. 2018), for example, a temperature of $<50^{\circ}\text{C}$, rather alkaline conditions, and a partial pressure of hydrogen $\log p\text{H}_2 > -5$. The time frame during which these conditions were present at Ceres is not well constrained. Obtaining this information for the current brine would help assess whether Ceres was habitable throughout its history.

Furthermore, access to Ceres' deep brine offers a unique opportunity to address many questions that pertain to most other ocean worlds, e.g., "What environments possess redox disequilibria, in what forms, in what magnitude, how rapidly dissipated by abiotic reactions, and how rapidly replenished by local processes?" (Hendrix et al. 2019). For example, several processes that enable the long-term availability or replenishment of chemical energy have been suggested. Although ocean worlds that evolve as closed systems may reach chemical equilibrium early in their history under an environment with high partial pressures of hydrogen resulting from serpentinization (Vance et al. 2016), various processes have been suggested for introducing oxidants into the ocean, including crustal breach and potential overturn via large impacts (e.g., Chyba 2000), release of fluids from the mantle as a result of thermal metamorphism (Melwani Daswani et al. 2021), or local water radiolysis driven by radioisotope decay (Altair et al. 2018; Bouquet et al. 2017). In Ceres, uranium and thorium may be present in rock particles that remained in suspension in the ocean, and potassium is expected to be abundant in the ocean as a result of rock leaching (Neveu et al. 2017; Castillo-Rogez 2020).

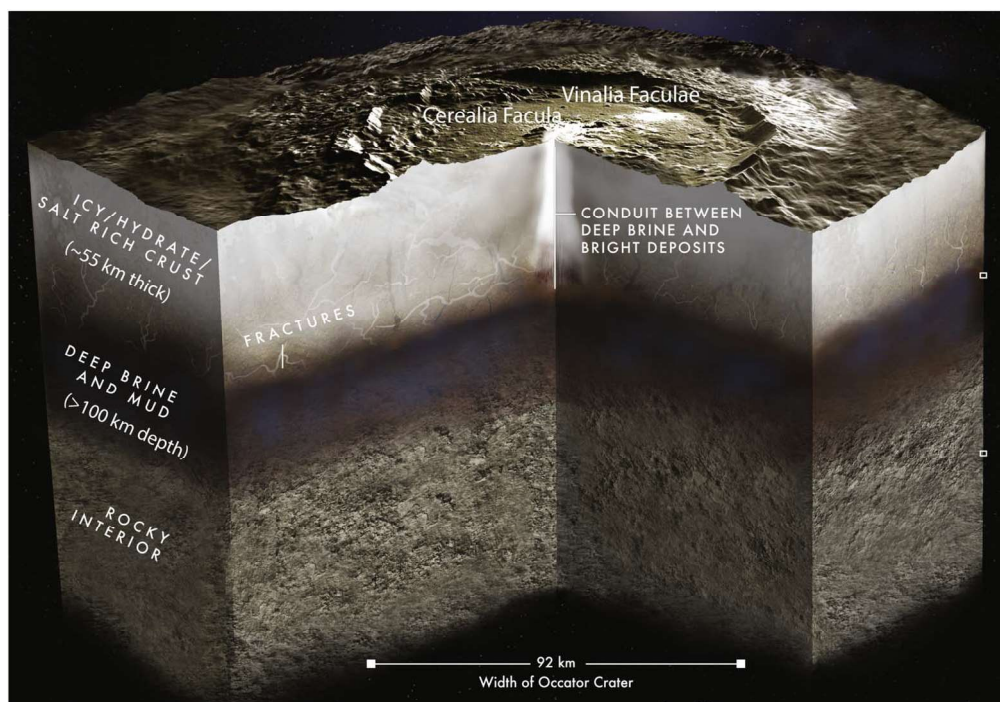


Figure 2. Geophysical context for the geological site investigated by this study. Medium-resolution imaging, compositional, and gravity data of the floor of Occator crater by the Dawn mission revealed the presence of a deep brine region that provides a long-lived source for evaporites found in Vinalia Faculae (Raymond et al. 2020; Scully et al. 2020; Nathues et al. 2020). A region of particular interest for a future sample return mission is Vinalia Faculae, located on the eastern part of the crater floor (see Section 3.4 for a detailed description of that region).

This objective is addressed by acquiring the full compositional inventory (mineralogical, elemental, and isotopic, including for minor species; organic compounds are addressed in objective 5) and analysis of the petrological relationships between mineral phases.

1.2.5. Objective 5: Characterize the Evolution of Organic Matter in Long-lived Brines

Ceres' regolith likely contains superchondritic concentrations of carbon (Prettyman et al. 2017, 2018; Marchi et al. 2019), and there is direct evidence for long-chain aliphatic compounds in patches found at Ernutet crater (De Sanctis et al. 2017) with less than 30% oxygen-rich functional groups (De Sanctis et al. 2019). However, information is lacking about the nature of that material and whether it was accreted early on, processed inside Ceres, and/or formed in situ.

In the context of ROW's "assess habitability" goal (Figure 1), determining the inventory of organic compounds falls under the theme of understanding the "availability (chemical form and abundance) of the biogenic elements, how does it vary throughout the ocean and time, and what processes control that distribution?" (Hendrix et al. 2019). The intent is to assess the sources, sinks, and stability of all solid organic compounds as potential feedstock for biochemistry and the cycles of major elements. For example, laboratory analyses of carbonaceous chondrites indicate that part of the soluble organic matter (SOM) tends to adsorb on silicates (Le Guillou et al. 2014). Hence, depending on temperature, a large fraction of SOM could settle with the rocky mantle during the differentiation phase. The dark material found in association with the Occator evaporites, which display a distinct aluminum-rich clay unique to that region, likely contains rocky material and organic matter that has evolved in the deep interior

(on top of regolith material) and can help assess the long-term evolution of organic compounds.

More generally, the evolution of accreted organic matter and potential for synthesis of new compounds on water-rich planetesimals are topics of major interest for understanding prebiotic systems (e.g., Vinogradoff et al. 2018). Future observations of Ceres' organic matter may be compared with organic compounds found in various carbonaceous chondrites (Vinogradoff et al. 2017) to quantify the change in the nature of abiotic organic compounds exposed to a long-lived deep ocean environment.

Organocarbonate relationships in evaporites would reveal diverse conditions driving the fate of carbon in ocean worlds, with the possibility of organic synthesis (e.g., Fischer-Tropsch type) or, alternately, degradation of the organics in an oxidizing environment (e.g., McSween et al. 2018). Both aspects have critical implications for framing the habitability potential of ocean worlds. Testing whether Fischer-Tropsch or other C1 reactions (e.g., electrochemical CO₂ reduction, etc.) occurred has critical implications regarding the production of hydrocarbons from accreted CO and CO₂. An important finding from the Dawn observations is that the two sites on Ceres that are sourced from the deep brine reservoir, the Occator faculae and Ahuna Mons, display abundant carbonate compounds with no evidence of organic matter at the spatial resolution of the Dawn infrared spectrometer (IRS; 10 and 100 m, respectively). This may indicate that organic matter has been degraded in the conditions of the residual brine, a hypothesis that has major implications for assessing the long-term habitability of ocean worlds.

These questions are addressed by studying the organic compounds expected to be trapped in the evaporite and in Occator's dark floor material. In terrestrial soda lakes, which are suggested to be analogous environments to Ceres' brine

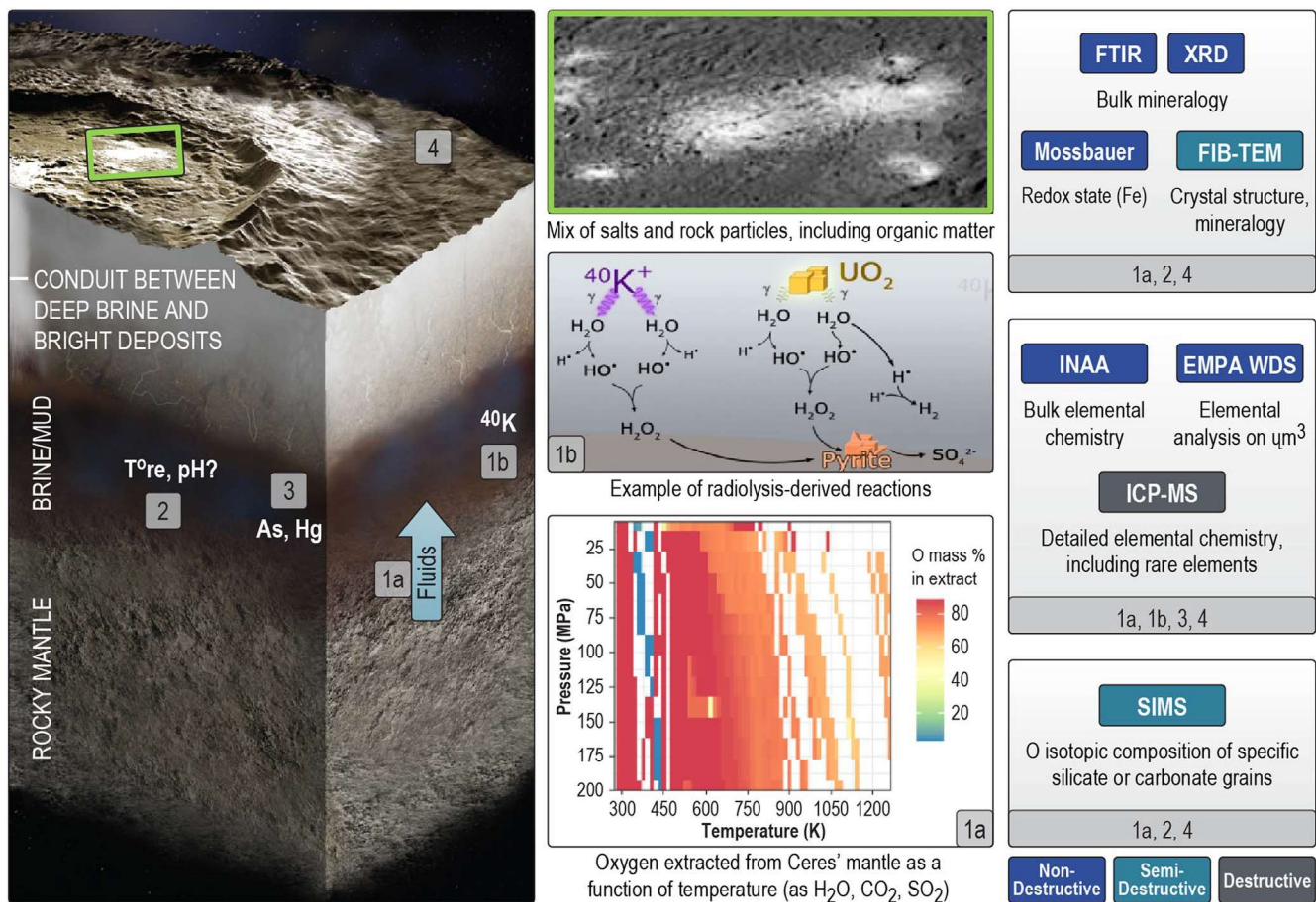


Figure 3. The characterization of Ceres' deep brine environment is addressed via a combination of elemental and mineralogical measurements and mapping of phase relationships. Possible techniques (among many others) are presented here: Fourier transform infrared (FTIR) spectroscopy and X-ray diffraction (XRD) for bulk identification of mineralogy; instrumental neutron activation analysis (INAA) for bulk elemental chemistry, followed by inductively coupled plasma MS (ICP-MS) for a more complete set of elements; electron microprobe wavelength dispersive spectroscopy analyses (EMPA WDS for chemistry) and fast ion beam–transmission electron microscopy (FIB-TEM for crystal structure/mineral identification) for detailed phase relationships; and secondary-ion MS (SIMS) for isotopic measurements on, e.g., carbonate oxygen. Numbers refer to testable hypotheses mentioned in the text. Left: Ceres cutaway produced by Raoul Ranoa. Top middle, NASA/JPL Caltech/UCLA/MPS/DLR/IDA; center middle, Altair et al. (2018); bottom middle: numerical modeling by Mohit Melwani Daswani (JPL).

region (Castillo-Rogez 2020), organic matter is found in carbonates (e.g., Benzerara et al. 2006). The two salt clasts (Zag and Monahans) found in collected meteorites also trapped organic species and a variety of other compounds, including fluid inclusions (Zolensky et al. 2017; Chan et al. 2018), on spatial scales of a few tens of nanometers.

1.2.6. Objective 6: Determine Ceres' Accretional Environment

Ceres' surface displays ammoniated clays and salts (De Sanctis et al. 2015; Raponi et al. 2019) and a large abundance of carbon, both of which have been interpreted as evidence for an origin of Ceres' volatiles in the outer solar system (De Sanctis et al. 2015; Marchi et al. 2019; Zolotov 2020). However, the ammonia has also been suggested to come from the thermal metamorphism of organic matter (McSween et al. 2018). Nevertheless, the source region of Ceres (e.g., Kuiper Belt versus Jupiter–Neptune; e.g., Gomes et al. 2005; Walsh et al. 2012; Raymond & Izidoro 2017) remains unknown. Furthermore, a massive proto-Ceres that formed in the main belt could accrete icy materials originating in the outer solar system via the mechanism of pebble accretion. In a gas-rich environment, small (centimeter- to meter-scale) building blocks may be transported via aerodynamic drag from the outer to the

inner solar system and accrete on massive planetesimals (Johansen et al. 2015). A caveat of this model is that these small blocks may lose volatiles as they cross the nebular gap opened by Jupiter (Turner et al. 2012), which may not be consistent with the accretion of ammonia in Ceres.

Many objects may be of interest for testing the origin of water in the inner solar system. Main belt comets in particular are associated with icy asteroids that may have preserved pristine ice (Meech & Raymond 2020). The interest in using Ceres for origin science stems from its large size, as it allows tests of whether 1000 km large planetesimals were present early on within the orbit of the giant planets, pebble accretion was indeed a major process in planetary formation, and large Kuiper Belt objects could be scattered and captured in the main belt of asteroids. Lastly, carbonaceous chondrite bodies have been suggested to be a major contributor to Earth's water (e.g., Budde et al. 2019) and a Ceres-sized body was potentially at the origin of a major impact at Mars (Canup & Salmon 2019).

Signatures of origin are generally found in elements and isotopes of volatiles and certain minor elements (e.g., Warren 2011; Kruijer et al. 2017). An example of a trade addressed during this study is whether constraints on origins are better approached by measuring isotopic ratios of volatile elements (O, N, H, C), which could be accomplished in situ, or

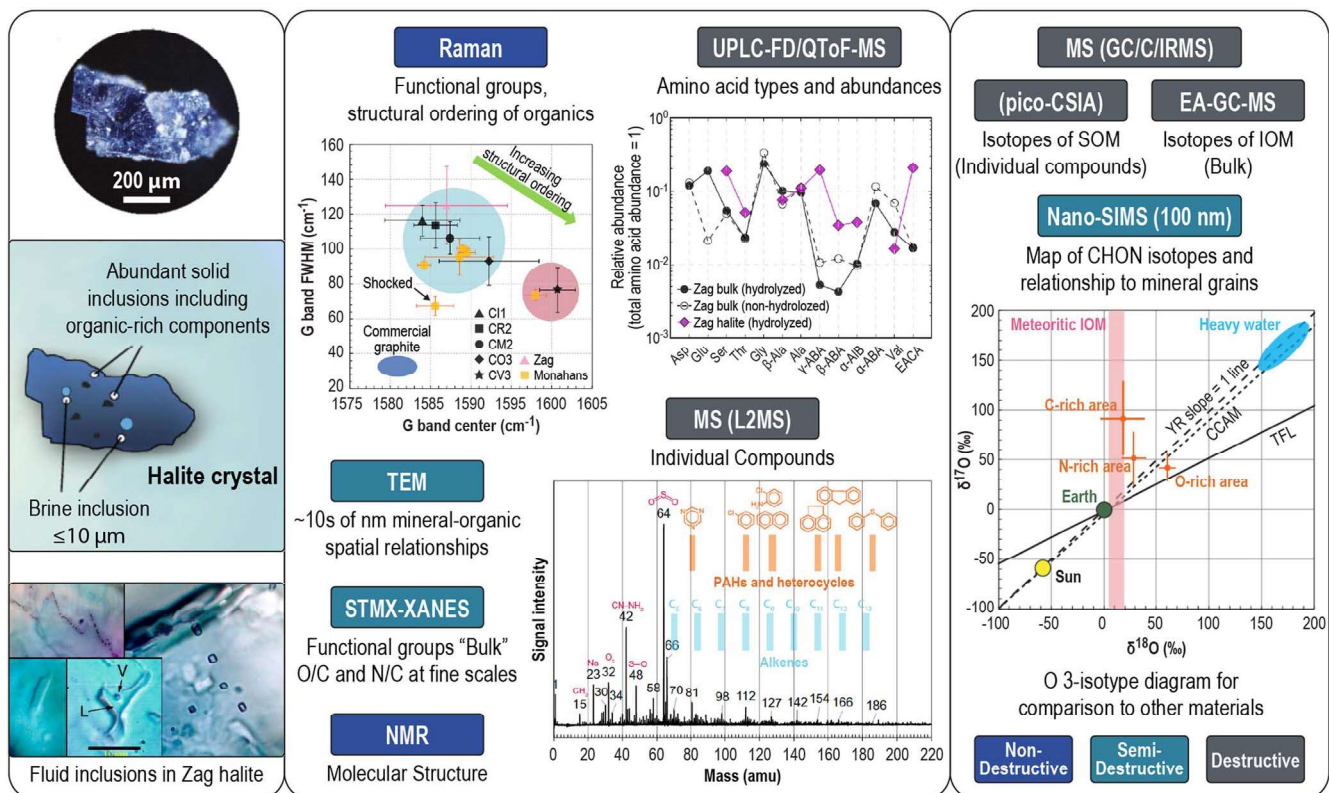


Figure 4. Characterization of organic matter that has been sitting in long-lived brines is addressed by a combination of elemental measurement; SOM and insoluble organic matter (IOM) characterization and relationships to minerals; and the isotopic composition of C, H, O, and N.; Raman spectroscopy to identify functional groups; nano-SIMS for spatial distribution of C, H, O, and N isotopes and relationship to mineral grains; transmission electron microscopy (TEM) for fine-scale (~tens of nanometers) mineral-organic spatial relationships and mineral identification; C, N, and O X-ray absorption near edge structure (XANES) for identification of organic functional groups and “bulk” O/C and N/C at fine scales; laser desorption/ionization MS (L2MS) for identification of individual compounds; ultraperformance liquid chromatography fluorescence detection and quadrupole time-of-flight hybrid MS (UPLC-FD/QToF-MS) for amino acids; for IOM isotopes, demineralization followed by elemental analyzer (EA) GC-MS (C+N) and thermal conversion EA-GC-MS; for compound-specific isotopic composition of soluble organics, GC combustion isotope ratio MS (GC/C/IRMS) or picomolar-scale compound-specific isotope analyses (pico-CSIA). Figures: Chan et al. (2018).

minor species (e.g., Cr, Ti), which requires terrestrial laboratories. Concerns were raised about the likely fractionation of these volatile elements as a consequence of hydrothermal processes and thus the erasure or alteration of the signature of origin, except maybe in the case of nitrogen (Li et al. 2009, 2012). On the other hand, the past decade has highlighted the significant information contained in minor elements, such as $\epsilon^{50}\text{Ti}$ versus $\epsilon^{54}\text{Cr}$ and $\Delta^{17}\text{O}$ ($\equiv \delta^{17}\text{O} - 0.52 \delta^{18}\text{O}$) versus $\epsilon^{54}\text{Cr}$, that highlighted the existence of separate reservoirs for carbonaceous and ordinary chondrites in the early solar system (e.g., Warren 2011). More generally, the theoretical framework for interpreting elemental and isotopic composition in terms of formation conditions in the solar nebula and the genetic relationships to the terrestrial planets is continually evolving. This drives the requirement to return a sample that can benefit from extensive analyses of minor species, whereas in situ measurements are necessarily limited in extent (see Section 1.4.2).

1.3. Science Traceability (Table 2)

1.3.1. Objectives 1 and 2

The search for ongoing activity at young geological features calls for medium-resolution imaging from orbit for comparison with images returned during Dawn XM2 ($\sim 5 \text{ m pixel}^{-1}$). The narrow-angle camera selected for landing site characterization can be used for this purpose. Gravity fields with a local degree strength up to 50 (which corresponds to a resolution of $\sim 25 \text{ km}$

or better) over regions of interest can be used to connect surface features to subsurface sources. This is achieved with radio tracking from $\sim 30 \text{ km}$ altitude, as demonstrated during Dawn XM2 (Park et al. 2020).

The remaining objectives require access to the surface. The focus on residual brines and organic matter led to the selection of Vinalia Faculae, on the floor of Occator crater, as the baseline landing region (Scully et al. 2021). The main part of Vinalia Faculae extends over $\sim 10 \text{ km}$ and thus offers many possible accessible sites based on the 5 m pixel^{-1} images returned by the Dawn mission (Scully et al. 2021).

1.3.2. Objective 3

The magnetotelluric method is preferred because joint measurement of electric and magnetic fields enables a complete sounding from a single station. Vinalia Faculae are hypothesized to overlay the deep brine region inferred from the Occator geologic observations (Figure 2) (Scully et al. 2020), which facilitates geophysical sounding. Modeling developed for this study (Grimm et al. 2020) shows that the response of brine in Ceres will be evident between 10^{-3} and 10 Hz . The ability to perform soundings over this frequency band can be determined from the joint signal-to-noise ratio of the magnetic and electric fields. The magnetometer and electrometer noise floors are taken from the Mars Atmosphere and Volatile Evolution (MAVEN) and Time History of Events and Macroscale Interactions During

Substorms (THEMIS) missions, respectively. The electrometer noise improves with increasing measurement baseline, and a 100 m deployment distance was specified and deemed feasible in the low-*g* Ceres environment, which yields 200 m baselines for a triangular configuration. Landed operations for 27 hr yield net signal-to-noise ratios >100 .

1.3.3. Objective 4

Testable hypotheses driving the analyses of evaporite materials include (Figure 3) (1) the existence of a chemical gradient as a result of (1a) past/ongoing flux of oxidants from the mantle and (1b) concentration of certain radioisotopes (Altair et al. 2018; Castillo-Rogez 2020), addressed via determination of the mineralogy (e.g., Castillo-Rogez et al. 2018), redox state of iron species, and search for radioisotopes; (2) environmental conditions (projected to be ~ 245 K and pH ~ 7 – 11) via a combination of mineralogy and isotopic measurements, in particular the thermometer $^{18}\text{O}/^{16}\text{O}$; (3) the possible concentration of elements harmful to life (e.g., certain metals); and (4) the rock composition for comparison with the regolith composition inferred from the Dawn data.

Basic understanding of evaporites and rocky composition can be obtained with in situ analyses combining Raman spectroscopy or mass spectrometry (MS), elemental spectroscopy (alpha particle-induced X-ray and/or gamma-ray and neutron spectroscopy), and isotopic measurements (either MS or tunable laser spectroscopy, TLS). However, the flight versions of these techniques remain limited by their coarse spatial resolution and thus their sensitivity to minor species, especially when it comes to estimating abundances (capability of tens of microns versus requirement of tens of nanometers for Raman spectrometers). Laboratory-grade facilities offer a 1 to several orders-of-magnitude increase in performance (e.g., spatial resolution of ~ 1 μm and detection limits of ~ 1 wt.% for Raman, depending on the species; e.g., Choukroun et al. 2021). Complementary measurements can be obtained to a much smaller spatial scale, like with a transmission electron microscope that can map mineral relationships on scales of tens of nanometers. Similarly, the context offered by medium spatial resolution mapping of elements and isotopes in a complex material is a major advantage of laboratory facilities over the bulk information obtained by in situ instruments.

In summary, Earth-based analysis of evaporite samples would also yield the high-precision isotopic, elemental, and mineralogical observations required to fully comprehend the first-ever brine sample returned from a planetary body and address future questions that may arise as the scientific framework for ocean worlds keeps evolving.

1.3.4. Objective 5

Earth-based analysis of evaporite samples would also yield the high-precision isotopic, elemental, and mineralogical observations required to meet this objective. Constraints on the origin of the organics can be achieved via the measurement of isotopic ratios, esp. $^{13}\text{C}/^{12}\text{C}$ and of their degree of maturation (e.g., H/C). The relationship between the organics and the salts, in particular the carbonates, can be addressed via various high-resolution phase-mapping techniques available only in Earth's labs (see also objective 4). A model of our approach is the comprehensive analyses performed by Chan et al. (2018) on the Zag clast (Figure 4). Organic compounds can be investigated in situ with a combination of Raman

spectroscopy or MS, elemental spectroscopy (alpha particle-induced X-ray and/or gamma-ray and neutron spectroscopy), and isotopic measurements (either MS or TLS). However, the perceived risk that organic compounds in bulk samples may be below the detection limits for state-of-the-art in situ instrumentation drives the need for a returned sample (see details in Section 2.3.2).

1.3.5. Objective 6

The isotopes necessary for this investigation require access to Earth-grade analytical facilities (Figure 5). Furthermore, origin science is an evolving field in terms of both the theoretical framework that isotopic and elemental ratios are compared against and finding the most informative combination of isotopic and elemental data. Hence, a sample return from Ceres' surface is required for this investigation to be successful.

1.3.6. Summary

A sample return of both the dark floor material forming the regolith and the evaporites (i.e., bright material from Vinalia Faculae) in Occator crater would enable the investigation of Ceres' materials using the next generation of Earth-based analytical facilities. Hence, this study focuses on this science implementation option.

At this point, we know of no other currently advocated ocean world sample return mission that would return an ~ 100 g sample acquired under nearly pristine conditions and preserved at cold temperatures ($\leq -20^\circ\text{C}$ required) until Earth return. For comparison, a sample return from Enceladus's tenuous plume would return <1 g of material (Tsou et al. 2012). An ~ 100 g sample would enable the planetary science and astrobiology community to take full advantage of the sample return curation and analysis capabilities currently being built up for Mars Sample Return; Origins, Spectral Interpretation, Resource Identification, and Security-Regolith Explorer (OSIRIS-Rex); Martian Moons eXploration (MMX); and Artemis samples from the Moon, placing Ceres sample return in series with a long line of planned sample return missions NASA is involved in. A sample of this size would enable analyses to benefit from improved analytical capabilities developed in the future.

1.4. Key Science Trades

The key trades performed to develop the mission concept are listed in Table 3. All of the major trades have been closed in order to drive to a point design necessary for the generation of a mass budget and spacecraft configuration used as input for costing. The study team recognizes that the conclusions identified in Table 3 do not represent the only possible way to accomplish this mission. It is quite possible that other teams evaluating the same trades would come to different conclusions.

1.4.1. Landing Site Trade

Based on the results from the Dawn mission, the following sites were also identified as being of scientific interest (Figure 6). This subsection summarizes the rationales that led to the selection of the Vinalia Faculae in Occator crater as the primary site for this study.

1. **Average surface.** Landing on the average surface of Ceres has the advantage that it does not require pinpoint (<20 m)

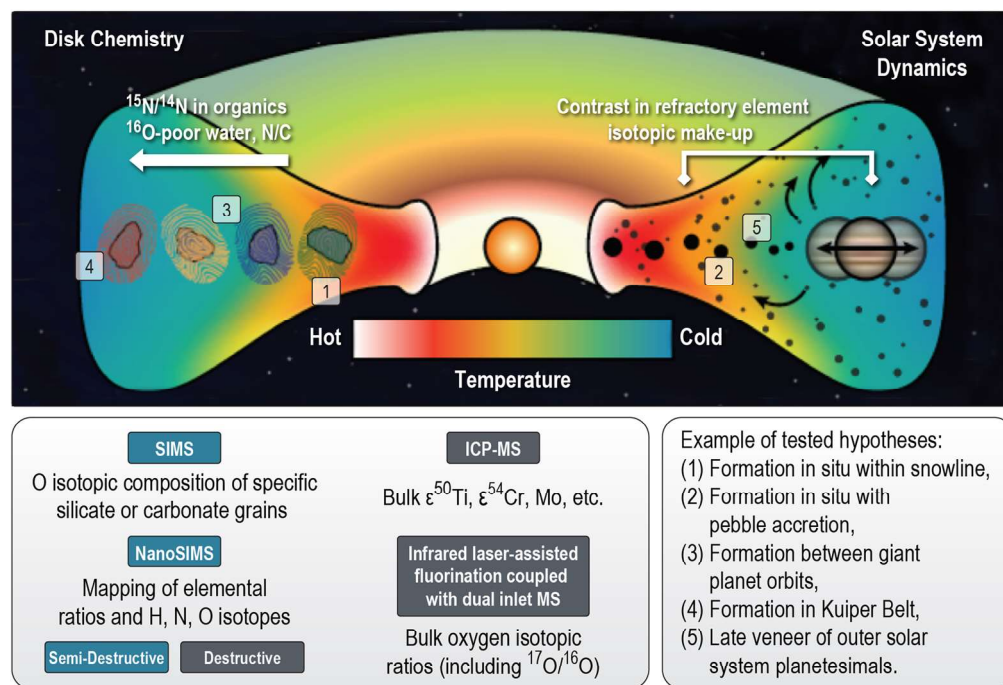


Figure 5. Hypotheses on the origin of Ceres can be tested by combining elemental ratios of light and heavy isotopes, such as bulk $\epsilon^{50}\text{Ti}$ and $\epsilon^{54}\text{Cr}$ via multiple collection ICP-MS, bulk oxygen isotopic ratios (including calculation of $\Delta^{17}\text{O}$) with infrared laser-assisted fluorination coupled with dual-inlet MS, secondary-ion MS (SIMS) for O isotopic composition of specific silicate or carbonate grains, and nano-SIMS for in situ analysis of, e.g., H, N, and O isotopic distribution. Based on Meech & Raymond (2020).

landing. The average regolith may contain superchondritic concentrations of carbon in various forms (Prettyman et al. 2018; Marchi et al. 2019) along with a mixture of salts and other aqueous alteration products. However, it has also been suggested that Ceres' regolith may contain up to 70 vol.% of exogenic material (Marchi et al. 2019; see also Vernazza et al. 2017) delivered by impactors and micrometeorites. As a result, investigation of the average surface of Ceres was considered scientifically risky. On the other hand, the sites of interest in Occator crater are less than 2 Ma and thus have barely been contaminated by infalling material.

2. **Ernutet crater.** This crater hosts kilometer-scale areas rich in organic matter, between 7% and 50% depending on the reference organic compound used for the interpretation of the Dawn infrared data (De Sanctis et al. 2017, 2019; Kaplan et al. 2018). Uncertainty remains about the origin of this material (endogenic or exogenic, e.g., from a small P- or D-type asteroid; Pieters et al. 2018). Furthermore, this site is dominated by average surface material that is likely to be heavily contaminated by infall. Hence, a mission targeting Ernutet crater would face the potential risk that a large fraction of the material investigated is of exogenic origin.
3. **Ahuna Mons.** The 4 km tall by 17 km long mountain was suggested, based on Dawn geophysical data, to stem from the briny mantle below the icy crust (Ruesch et al. 2019a). Furthermore, the emplacement of this large amount of material requires the presence of at least a small fraction of brines (Ruesch et al. 2016, 2019a). Hence, the investigation of Ahuna Mons material would provide an alternative way to address the habitability of Ceres' brine layer. However, a search for potential landing sites on Ahuna Mons revealed no viable, low-slope sites, leading to the necessity of landing adjacent to

Ahuna Mons and undertaking a remote-sensing investigation from the surface (Scully et al. 2021).

4. **Haulani crater.** This young (<2.5 Ma) crater has exposed material from the shallow (<5 km) crust and thus would offer an opportunity to probe the early ocean now frozen in the crust. Per its young age, the exposed material has been weakly weathered and contaminated by infall. However, a mission to that crater would uniquely focus on Ceres' early habitability, which was assessed by the science team and found to be less compelling for a follow-up mission to Ceres.

1.4.2. Sample Return versus In Situ Exploration

Measurement capability. For a concept focused on understanding Ceres' origin and current habitability potential, an in situ mission is limited by (1) the current performance of in situ instrumentation for organic matter characterization and isotopic measurements and (2) stringent contamination control requirements when looking for organics in very small abundance (nanogram). For instrument performance, we considered Raman spectroscopy and mass spectroscopy. For Raman spectroscopy, we considered the Compact Integrated Raman Spectrometer (PI: J. Lambert) developed under NASA's Instrument Concepts for Europa Exploration (ICEE-2) program. While that instrument's spectral range and resolution are particularly well adapted for science objectives targeting salts and organics, its spatial resolution of $\sim 10\ \mu\text{m}$ implies that it might not have sufficient sensitivity to detect organic compounds that may be on a scale of $< 10\ \text{nm}$, i.e., highly dilute, based on the Zag and Monahans clasts taken as reference (Chan et al. 2018). For mass spectroscopy, we assumed the next-generation ORganic Composition Analyzer (ORCA; PI: Chris Glein), also developed under the Instrument Concepts for Europa Exploration (ICEE-2) program. This model

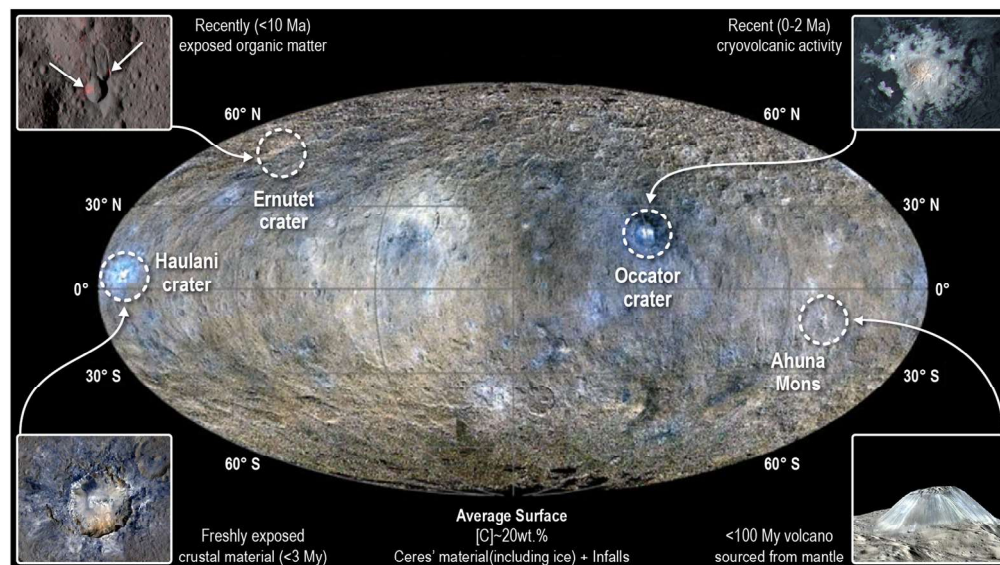


Figure 6. Five regions of high scientific value considered in this study. The PMCS science team concluded that Occator crater's evaporites offer the greatest opportunity to progress along the ROW.

has multiple front ends to separate the volatile and refractory components of planetary ices. However, discussion with the ORganic Composition Analyzer (ORCA) team indicated that this product would not be sensitive enough to detect organic compounds trapped in salt grains at the ppb level. ORganic Composition Analyzer (ORCA) has the capability to obtain the isotopic composition of Carbon, hydrogen, nitrogen, oxygen, phosphorus, sulfur (CHNOPS). However, a high-level issue identified during the team discussions is that origin science is complex and requires combining elemental ratios and isotopes of many volatile and heavy elements. Ultimately, the study team concluded that an in situ-only mission would not be able to address objectives 5 and 6. On the other hand, state-of-the-art instrumentation on Earth can achieve isotopic ratio measurements and organic detections by extracting and concentrating the materials of interest (see Figure 7).

Another major advantage of laboratory over in situ analysis is that various techniques can be employed to identify any form of contamination of the material. On the other hand, the in situ investigation of organics sets very stringent contamination constraints on the lander, sampling and transfer system, and instruments and is intrinsically limited in the diversity of techniques involved for assessing the organic matter makeup. A comparison of the science return expected for the in situ science and sample return concepts explored in this study is summarized in Table 4.

In summary, a sample return mission would benefit from a cumulative ~billion-dollar-level investment by NASA in facilities on Earth (NASEM 2019), as well as future investments, and engage a broad community in the analysis of the sample for several decades.

Single versus multisite exploration. A major advantage of the in situ concept is that it can reach at least two sites (one more after the first landing) for a moderate additional cost (see Figure 8). As hopping from one site to another is propellant-intensive, the PMCS team explored possible sites of interest separated by only a few tens of kilometers. The team converged on two sites located at Occator; the first site would be located in the dark ejecta material in the northeastern region of Occator (Homowo Regio), and the second one would be in the Vinalia

Faculae. Originally present in the shallow subsurface, the dark ejecta represents Ceres' early ocean material captured in the crust upon freezing. The composition of that material is significantly different from the average Ceres surface (Raponi et al. 2019). In particular, it is richer in ammonium salts. Its dark color is attributed to a fine grain size of tens of microns, which may represent fine particles forming the matrix of accreted planetesimals (Neveu & Desch 2015). Hence, the analysis of the composition (elemental, isotopic, and mineralogic) can be used to quantify the environmental characteristics and thus the habitability of Ceres' early ocean. A two-site mission targeting Occator crater ejecta and evaporites would then address Ceres' past and current habitability. With this combination of lander-accessible ancient and recent surface material, Ceres may be the only ocean world where this kind of information can be gathered. While this concept generated great interest in the study team, the potential risk of not identifying any organic matter with state-of-the-art in situ instrumentation led to the multisite architecture being rated as a second favorite.

1.4.3. Summary of Science Trades

For a similar cost and risk, a sample return from the Occator evaporites was deemed of greater scientific merit than an in situ mission targeting two sites. Both missions would capture objectives 1 and 2 in orbit and objective 3 in situ. On top of this, the sample return would both quantify the habitability of Ceres' brines and inform the fate of organic matter in ocean worlds (objectives 4 and 5). It would also enable long-term research on minor species and isotopes to determine the accretional environment of Ceres (objective 6). The in situ-only mission concept would address objective 4 but would not provide the spatial resolution and sensitivity required to characterize organic matter trapped in evaporite grains. It would also investigate a limited set of isotopes (volatiles only) that would allow only limited comparison with the volatile isotopic makeup of meteorites. However, a lander equipped with hopping capability could investigate a second site, for example, the northeastern ejecta region of Occator crater (Homowo Regio), made of crustal material and acquire additional information on

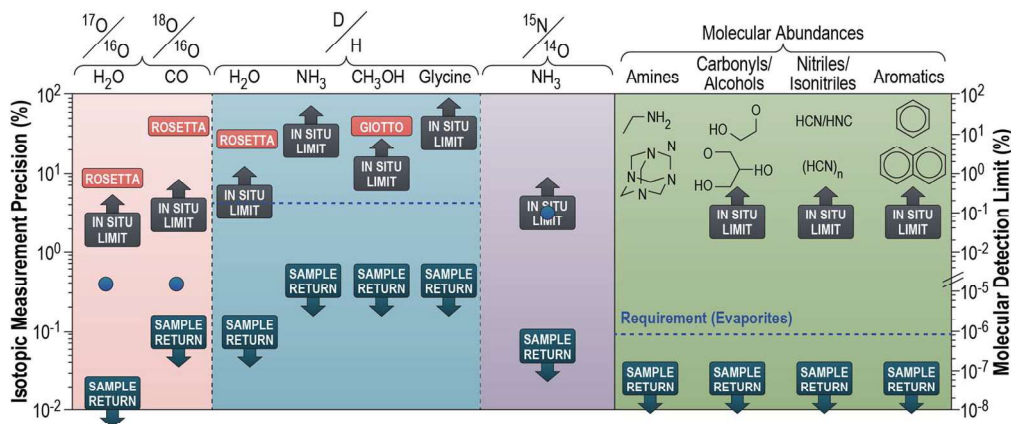


Figure 7. Performance comparison between in situ measurement and Earth's laboratory measurement techniques against measurement requirements (blue circles and lines). The requirement to measure $^{17}\text{O}/^{16}\text{O}$ and determine the nature of the organic compounds believed to be highly diluted drives the need for high-grade facilities. Initial isotopic ratios depend on the mineral in which the reference element is incorporated (e.g., Willacy & Woods 2009 for D/H). Although high-precision D/H can be measured in water with in situ payload, material ingestion techniques cannot separate minerals, resulting in a signal that is diluted and difficult or even impossible to interpret reliably. Based on Milam et al. (2021).

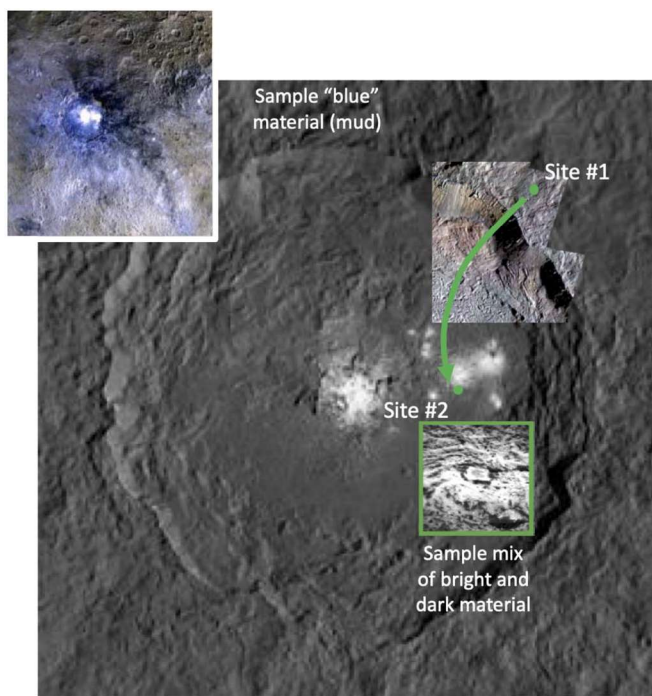


Figure 8. Two landing regions identified as being of high value for the in situ concept: Homowo Regio (Occator crater northeastern ejecta) followed by Vinalia Faculae. The two regions are separated by about 40 km.

Ceres' early oceanic environment and organic matter. The characteristics and projected science for the sample return mission concept are further compared to that for the in situ concept and summarized in Table 5.

2. Science Implementation

2.1. Strawman Payload for Sample Return Mission

The strawman payload includes a narrow-angle camera for medium- and high-resolution imaging of geological landmarks and landing site contextual characterization and certification prior to landing. Indeed, the highest imaging resolution returned by the Dawn mission at the Vinalia Faculae is 25

times too crude to support the identification of safe landing sites.

The spacecraft includes body-mounted context cameras for characterization of the landing site following landing. These are considered engineering cameras, included under the flight system. The landed phase uses an in situ IRS for characterization of the sampled material, in particular to quantify its degree of hydration prior to return to Earth.

The second instrument used in situ and the main in situ science investigation is a combination of magnetometer and electrodes.

2.2. Infrared Point Spectrometer

This instrument (Table 6) covers the spectral range from 2 to 4 μm that encompasses carbonate, organic functions, and water signatures. Its spectral resolution of 10 nm is adequate for the resolution of the various forms taken by water (ice, hydration, hydroxyl).

This instrument is based on a new generation of low-mass, low-power IRSs developed at JPL for CubeSat/smallsat applications (Ehlmann et al. 2019) and is priced as a Class B instrument. The IRS is body-mounted and would be used to characterize the landing site. It requires a cryocooler to keep the focal plane array at $<100\text{ K}$. The cryocooler is turned on for 4 hr prior to data acquisition. Deployable covers are included in the design in order to prevent optics contamination upon landing.

The data returned are in the form of a spectral cube. The instrument does not include any flight software. Only a few images are needed to characterize the working space, obtained at different times of the day for an estimated total of 6 Gb. Data analysis is low complexity and relies on spectral fitting using, e.g., the Reflectance Experiment Laboratory database. Narrowing down to a specific mixture composition can be a laborious process but builds on long-time expertise by various groups.

2.3. Magnetotelluric Sounder

The Ceres Magnetotelluric Sounder (Table 7) determines the depth-dependent electrical conductivity of the subsurface from frequency-dependent magnetic and electric fields. This instrument is—to within the fidelity of a concept study—identical to

the Lunar Magnetotelluric Sounder developed at the Southwest Research Institute (PI: Robert Grimm) and selected for lunar flight on the CLPS (Commercial Lunar Payload Services) 19D mission.

The four electrodes are deployed at 90° azimuths, and the mast is deployed vertically. Deployments from the electrode launchers are a one-time activity developing over 5 minutes at 30 W. The source signal is specified as the magnetic field spectrum of the solar wind near the Earth, scaled to the distance of Ceres. The electric field due to induction is calculated from the model response for different assumptions on brine conductivity (1–10 S m⁻¹) and depths (>35 km). Preliminary modeling indicates that brines can be detected by measuring ambient electric and magnetic fields over 3 Ceres days (~27 hr) for a data volume of <1 Gbit.

The electrode deployments to 100 m enable a baseline of 200 m to guarantee probing down to >50 km. This means that if the brine layer is less than 25 km thick, the interface with the mantle could be detected. Furthermore, the 2.5 m high mast stands off the magnetometer to alleviate any spurious magnetic signals produced by the spacecraft. Any remaining spacecraft noise identified by ground testing, analysis, or experience would be dealt with via relatively common techniques, such as backwiring solar arrays, magnetically shielding individual components, and/or using operational knowledge to correct or ignore corrupted data. In this way, an experienced team (both spacecraft and instrument) could eliminate any magnetic cleanliness issues with modest effort. This approach has been successful on numerous previous missions (e.g., MAVEN, Juno, etc.).

The instrument has one operational mode with a few settings (sample rate, electrometer gain). Returned data are time series of the electric and magnetic (B) fields. Data analysis requires editing, filtering, fast Fourier transform, calculation of impedances (E/B complex transfer functions), 1D inversion to conductivity-depth structure, and geological interpretation.

2.4. Curation and Handling

The sample curation and analysis component of this concept was developed following the guidelines of the Planetary Science Decadal Survey provided by the National Academy of Sciences, Engineering, and Medicine (NASEM 2020), “Studies of meteorites and other extraterrestrial materials in terrestrial laboratories that further planetary science goals are in scope but findings and recommendations in this area should take into consideration the National Academies report Strategic Investments in Instruments and Facilities for Extraterrestrial Sample Curation and Analysis (2019).”

The sample curation laboratory would be designed, constructed, and completed at least 1 yr prior to sample return. This would be an organically clean, ISO 5 cold curation facility whose design would take full advantage of 50 yr of astromaterial curation experience at Johnson Space Center (JSC) and by other institutions in the United States and internationally.

The sample return capsule (SRC) will return to the Utah Test and Training Range (UTTR), where it will be collected and stored in a temporary clean room before being transported to JSC for permanent curation of the returned samples. A maximum of 25% of the returned sample will undergo preliminary examination (PE; Figure 9). Contamination knowledge witness plates and portions of spacecraft hardware will

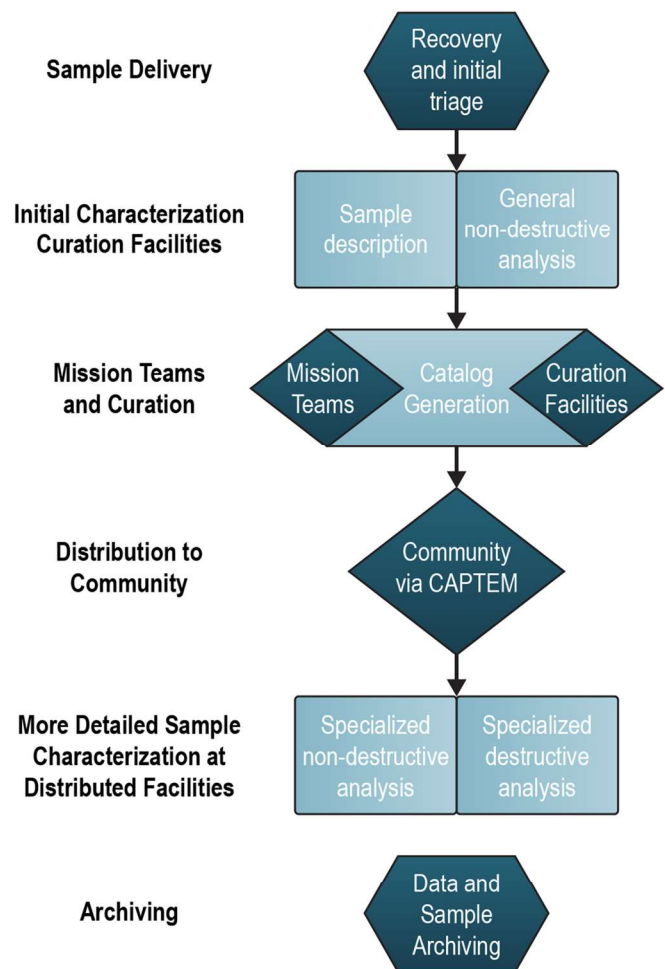


Figure 9. Returned sample processing flowchart. Source: Curation and Analysis Planning Team for Extra-Terrestrial Material (CAPTEM), now the Extraterrestrial Materials Analysis Group (ExMAG). See NASEM (2019).

also be subdivided and allocated for analysis during and after sample PE. The main goals of sample PE are to establish the basic nature and state of the collected samples, develop a sample database for the planetary science community, and elucidate any sample contamination.

The number of laboratory analyses planned during sample PE is derived from the many measurements sought in Table 2, some of which are destructive and semidestructive (Figures 3–5), and the expectation that similar measurements may be carried out by different groups for reproducibility purposes. This leads to a sample mass requirement of ≥ 100 g. The mission plan prioritizes surfaces without exposed ice and with unconsolidated material, further increasing the likelihood of collecting ≥ 100 g of nonvolatile material. Analytical techniques in Earth-based laboratories measure the organic, elemental, isotopic, mineralogical, petrological, and spectral characteristics of the pristine samples in extraordinary detail, addressing the key mission science. This mission utilizes analytical techniques available at the time of sample return, many of which are likely yet to be developed, as was the case for Stardust, Hayabusa, etc. The PE period is 2 yr, and, per NASA guidelines, $\leq 25\%$ of the returned sample is employed for PE investigations, leaving $\geq 75\%$ of the returned material for long-term curation to permit future investigations.

Table 2
Science Traceability Matrix for a Sample Return Mission from Occator Crater's Mixed Evaporite and Floor Material

Science Objective	Measurement	Instrument Requirements	Functional Requirements
O1. Test whether extrusion from a brine-rich mantle occurred during Ceres' recent history. Addresses the "energy sources" and "chemical gradients" objectives in ROW (Figure 1).	<ol style="list-style-type: none"> 1. Imaging in the visible and two color filters with a spatial resolution of $<5 \text{ m pixel}^{-1}$ to search for geological structure (exploratory). 2. Spacecraft acceleration via Doppler shift at 25 km half wavelength. 	<ol style="list-style-type: none"> 1. Narrow-angle camera with two color filters (plus clear), e.g., $450 \pm 20 \text{ nm}$ (blue) and $850 \pm 20 \text{ nm}$ (red), iFOV of $10 \mu\text{rad}$. 2. Telecom subsystem (X-band); no additional hardware required. 3. DSN Doppler accuracy: $\leq 0.1 \text{ m s}^{-1}$ for 60 s integration time. 4. Transponder stability $\leq 10^{-13}$ at 1000 s. 	<ol style="list-style-type: none"> 1. Polar orbit, altitude $<500 \text{ km}$ for imaging. 2. 14 Gbit. 3. Polar orbit, altitude $<30 \text{ km}$ for radio science; two-way coherent Doppler tracking. 4. Successive passes offset by $\sim 1^\circ$ to map targets of interest. 5. Target Occator, Haulani craters; Ahuna Mons, Cosecha Tholus.
O2. Test whether endogenic activity is ongoing at Occator crater. Addresses the "energy sources" and "chemical gradients" objectives in ROW.	<ol style="list-style-type: none"> 1. Imaging in the visible and two color filters with a spatial resolution of $<5 \text{ m pixel}^{-1}$ for comparison with images returned by the Dawn mission. 	<ol style="list-style-type: none"> 1. Narrow-angle camera with two color filters (plus clear), e.g., $450 \pm 20 \text{ nm}$ (blue) and $850 \pm 20 \text{ nm}$ (red), iFOV of $10 \mu\text{rad}$. 	<ol style="list-style-type: none"> 1. Observe Occator crater from polar orbit from $<500 \text{ km}$. 2. 3 Gb (2 Gb of visible imaging included above).
O3. Determine the depth of liquid water below Occator crater. Addresses the "rock/ocean Interface" and "chemical gradients" objectives in ROW.	<ol style="list-style-type: none"> 1. Electrical conductivity to $>50 \text{ km}$ depth (brine expected from 35 km depth). 	<ol style="list-style-type: none"> 1. Electric field (electrodes) $1 \mu\text{V m}^{-1}$, magnetic field (magnetometer) 0.1 nT (magnetotelluric method). 	<ol style="list-style-type: none"> 1. Deploy at Vinalia Faculae. 2. Integrate for 50 hr (27 hr required + margin). 3. Data volume: 600 Mbit.
O4. Characterize Ceres' deep brine environment at Occator crater. Addresses the "solvents", "chemical gradients" and "Physico-Chemical Conditions for Life" objectives in ROW.	<ol style="list-style-type: none"> 1. High-precision ($<1\%$) and spatial resolution (submicron) mineralogy, including phase relationship mapping between minerals. 2. Spatially resolved elemental composition. 3. Spatially resolved C, H, O, N, isotopic composition. 	<p>Mineralogy – See Figures 3, 4, 5.</p> <ol style="list-style-type: none"> 1. X-ray diffraction, Mössbauer spectroscopy. 2. Raman spectroscopy to detect materials in relative abundance of $>1 \text{ wt.}\%$. <p>Elemental Composition.</p> <ol style="list-style-type: none"> 1. XANES and carbon-XANES. 2. INAA. <p>Organic compounds.</p> <ol style="list-style-type: none"> 1. Nuclear magnetic resonance spectroscopy. 2. Amino acid analysis, UPLC-FD/QtoF-MS. 3. EA-GC-MS, pico-CSIA. <p>Isotopes:</p> <ol style="list-style-type: none"> 1. MS (various techniques depending on the material). 2. Nano-SIMS. 3. ICP-MS. 	<ol style="list-style-type: none"> 1. Sample a mixture of bright (evaporite) and dark material at Vinalia Faculae. 2. Sampling of surficial material. 3. Sample mass: 100 g, driven by the use of destructive analysis techniques (tens of mg and up to 1 g of sample per analysis). 4. Particulate contamination control to ISO 5 and nonvolatile organic residue limited to level A/2; return at $\leq -20^\circ \text{ C}$ to prevent water vapor release that would drive salt deliquescence and potential aqueous alteration in the SRC. 5. No requirement to preserve the stratification of the sample. 6. Prevent atmospheric leakage into the SRC during and after Earth entry until SRC recovery; maintain internal pressure $<3 \times 10^{-5} \text{ Pa}$ after SRC closure through SRC recovery. 7. Storage at $<-80^\circ \text{ C}$. 8. See Figure 9 for sample processing flowchart.
O5. Characterize the evolution of organic matter in long-lived ocean. Addresses the "inventory of organic compounds" as environmental markers and potential feedstock in ROW.	<ol style="list-style-type: none"> 1. Elemental composition and nature and quantification of organic compounds and relationship to minerals (submicron scale). 2. Isotopic composition of C, N, O, H with accuracy and precision $<1\%$. 	<ol style="list-style-type: none"> 1. Nuclear magnetic resonance spectroscopy. 2. Amino acid analysis, UPLC-FD/QtoF-MS. 3. EA-GC-MS, pico-CSIA. 	
O6. Determine Ceres' accretional environment. Addresses the connection between Ceres, icy moons, and/or dwarf planets and puts the results of objectives 1-5 in greater context.	<ol style="list-style-type: none"> 1. Elemental and isotopic ratios of volatile elements (e.g., H, N, O) and refractory minor species (e.g., $\epsilon^{50}\text{Ti}$ versus $\epsilon^{54}\text{Cr}$ and $\Delta^{17}\text{O}$ versus $\epsilon^{54}\text{Cr}$) with $<1\%$ accuracy and precision. 	<ol style="list-style-type: none"> 4. All three objectives require visible and in situ infrared imaging of the landing site for context and to assess the level of hydration of the material prior to its dehydration during return to Earth. 	

Note. The overarching goals of this concept are to (1) assess Ceres' current habitability and use Ceres as a test case for determining the habitability of volatile-rich bodies over time (objectives 1–5) and (2) determine Ceres' origin and the relationship of its volatiles and organics to other inner solar system bodies (objective 6). The mission payload is limited to a narrow-angle camera and electromagnetic sounding package needed to address Objectives 1-3, and a point spectrometer used for in situ characterization of the sampling area. Objectives 4-6 use measurements with instrumentation available in terrestrial facilities. See Figures 3–5 for a definition of the instrument acronyms. Here, iFOV is instantaneous field of view.

Table 3
Key Trades

Key Trades Performed	Outcome	Rationale
Selection of scientific site (among five downselected)	Occator crater evaporite (Vinalia Faculae)	Occator crater displays freshly exposed evaporites, which offer direct insights into the habitability of Ceres' residual ocean and would allow testing of the occurrence of a number of processes predicted to take place in ocean worlds (see Figures 1, 3, and 4).
Sample return versus in situ exploration	Sample return option preferred	Sample return enables searching for minor phases, including organic compounds, that may not be detectable with state-of-the-art in situ instruments, along with some in situ science for sample context characterization (see Table 4 and Figure 7).
Single spacecraft versus orbiter + lander	Single spacecraft using SEP for cruise and hydrazine thrusters for landing and takeoff	Single spacecraft expected to be lower cost than two major flight elements because of single avionics, telecom, power, thermal systems.
Sample acquisition via legs versus deployable arm	Acquisition via legs	Sampling at discrete leg locations has less operational complexity than sampling from a deployed arm and would collect the necessary amount of material from the assumed weak surface; collecting samples from locations other than the lander footpads would not be necessary to achieve science goals.

Since a major objective of this concept focuses on organic science, extra precautions should be applied to contain potential organic contamination while the samples are exposed to the terrestrial environment following return. A mission contamination knowledge campaign will include monitoring witness materials during curation analyses to track the types of abundances of contaminants accumulated over time. Lessons can be learned from previous and ongoing sample return missions (e.g., see Chan et al. 2020 for a review; Dworkin et al. 2018 for OSIRIS-REx; McCubbin et al. 2019 for Stardust).

The mission team should apply state-of-the-art contamination control protocols, for example, analysis in a class 100 (i.e., ISO 5) clean laboratory. However, a review of lessons learned from past sample return missions by Chan et al. (2020) shows that contamination cannot be avoided. Fortunately, most terrestrial organics can be identified with laboratory techniques based, for example, on their isotopic and molecular characteristics (see Chan et al. 2020 for more detail). Techniques such as etching the surface of the studied grains with an ion beam can remove contaminants prior to analysis (e.g., Koike et al. 2020). Furthermore, Cerean organics trapped in salt grains would be protected from terrestrial contamination and remain uncontaminated when studied in a class 100 clean lab (e.g., Chan et al. 2018; Koike et al. 2020). Organic compounds collected from the dark floor material are expected to be abundant (Prettyman et al. 2018) and share distinct relationships with the rocky material.

Another essential requirement of the mission contamination assessment and control plan will be to preserve the witness surfaces indefinitely and also preserve (document and curate indefinitely) samples of all spacecraft materials that have any potential to contact samples, including by outgassing. The curation facilities will have identical requirements.

3. High-level Mission Concept

In this section, we summarize the technical implementation aspects of this concept. More details on the flight system and mission design can be found in Brophy et al. (2022), landing site selection and accessibility is addressed in Scully et al. (2021), and planetary protection considerations can be found in Castillo-Rogez et al. (2021).

3.1. Overview

The total ΔV for a round-trip sample return mission to Ceres is approximately 14 km s^{-1} , which could be achieved through the use of solar electric propulsion (SEP). In comparison, the ion propulsion system on the Dawn mission provided a total ΔV of 11.5 km s^{-1} . An additional 600 m s^{-1} would be required to land on and take off from the surface of Ceres. A monopropellant hydrazine propulsion system would be adequate for this. An example round-trip, low-thrust trajectory is given in Figure 10 for a 2030 December launch. The use of SEP would enable a launch any year from 2030 through 2037 with little change in the flight time, launch mass, and propellant mass. The total flight time would be about 13 yr: ~ 6.7 yr to get to Ceres, 500 day stay time at Ceres, and 4.7 yr to return the sample to Earth.

The sample return mission concept was developed to concept maturity level 4 resulting in a detailed master equipment list, concept of operations, and driving power modes. Detailed low-thrust trajectory analyses were used to determine the required solar array size and electric thruster type. Deorbit, descent, and landing analyses were used to determine the amount of hydrazine propellant needed to land in Occator crater. Similar analyses were performed to determine the propellant required to return to Ceres orbit. A single flight element, referred to as the SEP lander, shown in Figure 11, would be used to perform these functions.

The mission would begin with the launch on a high-performance launch vehicle with a 5 m fairing. The performance of the Falcon Heavy recoverable launch vehicle was used in the trajectory analyses. The spacecraft would be launched from Kennedy Space Center (KSC) to a C3 of approximately $13.4 \text{ km}^2 \text{ s}^{-2}$. Most of the 500 days at Ceres would be spent in orbit, identifying and characterizing landing sites as part of the landing site selection process (see Scully et al. 2021) and performing orbital science. Note that this duration includes a 30% margin and time on the ground to process the data and select the landing site via a community-led process.

The solar arrays would be retracted and stowed for landing. A throttleable hydrazine propulsion subsystem would be used to deorbit the spacecraft from a 28 km altitude orbit and land it in Occator crater at the Vinalia Faculae. An enhanced lander

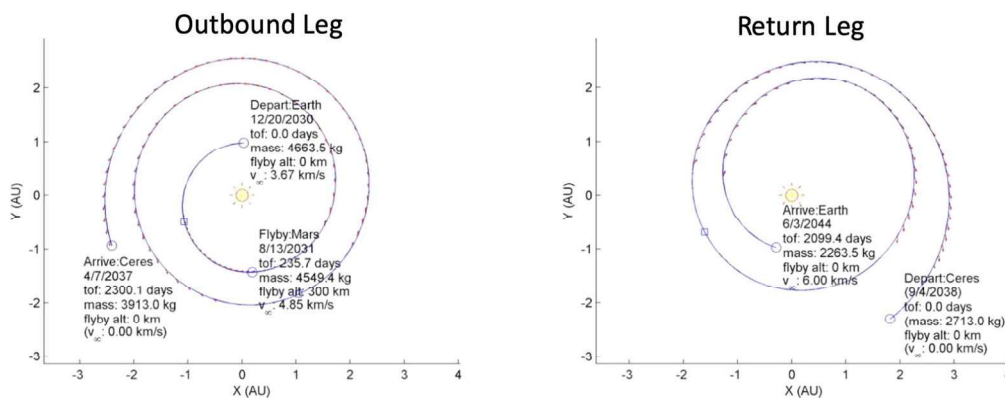


Figure 10. Example trajectory for the outbound and return cruise phases for a 2030 launch. With SEP, sample return missions can be launched in any year from 2030 through 2037 with little change in performance. For example, a 2033 launch decreases the total flight time from 12.8 to 12.6 yr and increases the Earth arrival mass from 2264 to 2269 kg. A Mars gravity assist flyby and stay time of 500 days at Ceres are included in all cases.

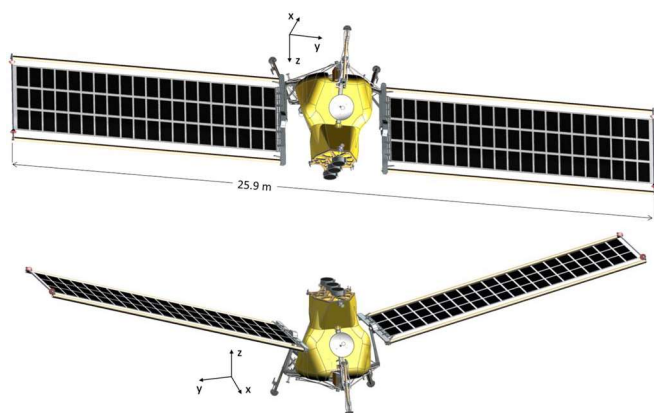


Figure 11. The SEP lander spacecraft in the cruise configuration (top) and the landed configuration (bottom). In the cruise configuration, the solar arrays are articulated about the y -axis to track the Sun during thrusting with the electric propulsion system. A second axis of articulation about the x -axis reduces the risk of the arrays contacting objects on the surface of Ceres in the landed configuration.

vision system would be used to provide altimetry, velocimetry, and terrain-relative navigation to guide the spacecraft to the preselected safe landing site. The solar arrays would be redeployed after landing and provide ample energy over the course of each Ceres day (~ 9 hr) to operate the flight system on the surface. The solar arrays would have a second axis of articulation that increases the clearance between the solar array wings and the surface after deployment, as suggested in Figure 11.

A sample acquisition system derived from that being developed for the JAXA MMX sample return mission would be used to collect material from the surface. There would be one sampling system in each of the three lander legs for robustness. Each sampling system would pneumatically deliver the acquired samples directly to the SRC. Sampling would be verified optically during sample collection.

After successful sample acquisition, the solar arrays would be retracted and stowed a second time for takeoff. The hydrazine propulsion system would take the vehicle off from the surface and return it to a 28 km altitude Ceres orbit. Once back in orbit, the solar arrays would be redeployed for the third and final time. The SEP system would be used to depart from Ceres orbit and perform the heliocentric transfer back to Earth. The trajectory would be designed to release the SRC with a

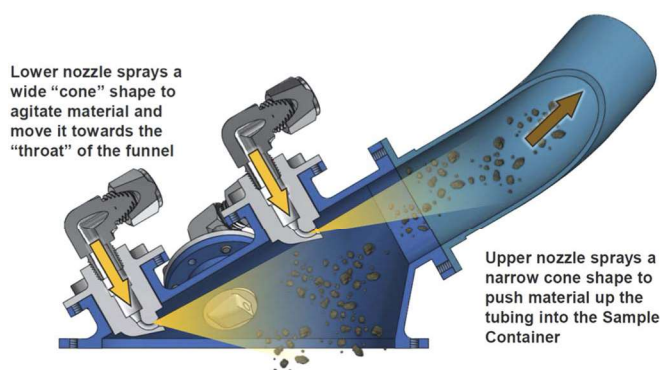


Figure 12. Example PlanetVac-type sampler. Compressed gas is used to lift loose surface material and transport it through a long tube leading to the sample container in the SRC. From Zacny et al. (2019).

hyperbolic excess velocity (V_∞) of ≤ 6 km s^{-1} and target landing at the UTTR. After release of the SRC, the spacecraft would perform a divert maneuver. The SRC would be recovered at UTTR and the samples transferred to the Astromaterials Acquisition and Curation facility at JSC.

The sample acquisition system would utilize the pneumatic PlanetVac technologies (Figure 12) for collection of materials from the surface of Ceres and transfer to the SRC for return to Earth.

This system would use gas flow sourced from a compressed gas cylinder (N_2) to move grains for both collection and transport from the Ceres surface to the SRC. The sampler for a conceptual Ceres sample return mission is derived from TRL 6 PlanetVac systems developed for multiple atmosphere-free planetary-body applications (Zacny et al. 2020), including the JAXA MMX mission NASA sampler contribution, as well as from the Dragonfly mission. Scully et al. (2021) assessed the prospect for and properties of safe landing sites in the Vinalia Faculae region. The current state of understanding is that material was primarily emplaced via ballistic venting of brines, but exposure via effusion is also possible (see also Ruesch et al. 2019b). Hence, augmentation of the pneumatic sampler with a drill or other device to mechanically break apart the surface was also considered for increased robustness to a wide range of ground strengths (see Zacny et al. 2019 for more detail). The sampling system considered was demonstrated to drill down to 2 cm depth. Since the material was recently exposed, it has been subjected to little space weathering: ultraviolet radiation

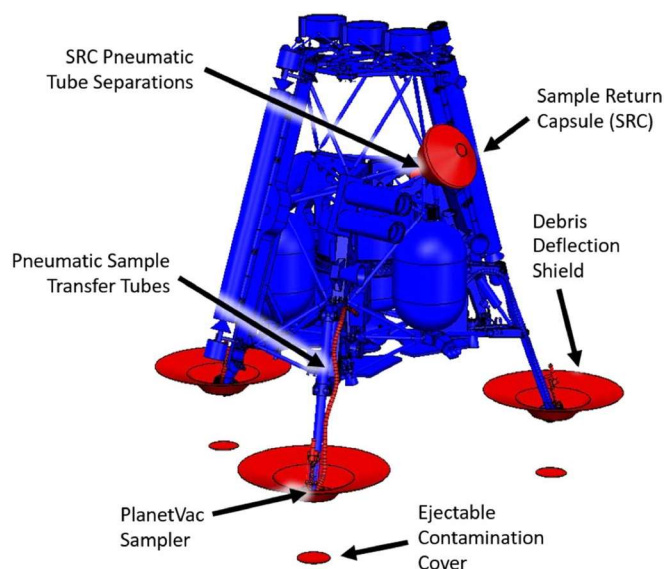


Figure 13. Sample chain elements shown in red.

rapidly affects only the first 100 μm ; solar energetic protons and galactic cosmic rays (GCRs) can reach material over a greater depth, but it takes these particles \sim tens of megayears to significantly alter material over a few centimeters (Nordheim et al. 2021); and recent/ongoing infalls might contaminate the material over depths of 0.1–1 mm (Costello et al. 2021). Hence, there is no requirement to drill deep below the surface to find pristine material.

For the science objectives listed above, there is no requirement to preserve sample stratification. The latter would inform on emplacement mechanisms. However, geological context has already provided extensive information on the topic (e.g., Ruesch et al. 2019b), and magnetotelluric sounding will provide complementary information on geophysical context. As noted above, space weathering due to ultraviolet radiation, solar energetic protons, and GCRs would alter the first millimeters of the surface material after exposure and only partially degrade organic compounds (e.g., Nordheim et al. 2021 and references therein). Laboratory analysis would help sort out those grains, and comparisons between weathered and unweathered material would bring new insights into the effect of space weathering at airless bodies. Note, however, that the latter investigation is not part of the objectives defined for this sample return concept, since it is not possible to date the exposure of the sampled materials (i.e., they could be very recent and weakly affected by space weathering, if not at all).

The configuration of the conceptual sample chain elements is illustrated in Figure 13. Key aspects include PlanetVac sampler heads integrated into each of the three lander footpads in a fixed location, debris deflection shields to direct sampling-induced debris on a ballistic path away from the spacecraft, pneumatic transfer tubes to carry the sample to the sample container located in the SRC, and the SRC pneumatic tube separation mechanism. Protection from contaminants during the outbound cruise is provided by ejectable contamination covers over the sampler collection heads.

3.2. Sample Return Capsule

The SRC assumes the same capability as that used successfully on Stardust and OSIRIS-REx. Internal modifications would be made for the delivery of the sample material to

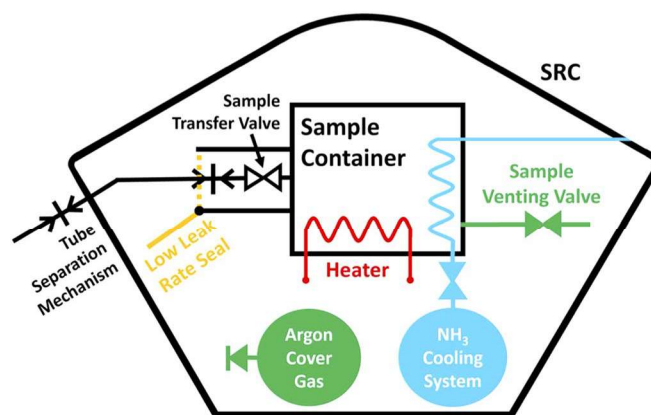


Figure 14. Conceptual SRC sample containment system architecture.

the SRC and to maintain the samples in the desired environment for delivery all the way to UTTR. The SRC includes an aeroshell with an ablative thermal protection system, a backshell, avionics, and the mechanisms to close and seal the sample delivery tubes. The SRC would be a passive, spin-stabilized capsule that would use a parachute system to land. A mechanism mounted on the spacecraft bus would generate the required spin and separation rates. A preliminary assessment by NASA Langley has confirmed that the reentry conditions targeted by the low-thrust trajectories would result in stress and thermal loads within the capability of the Stardust SRC (T. White 2020, personal communication).

Function requirements for the sample container are shown in Table 8. An approach to meeting these requirements using the sample container technologies of TRL 6–9 was identified that employs three main elements: argon cover gas, an ammonia cooling system via compressed gas expansion, and a low leakage rate seal (10^{-10} Pa m^{-3} s^{-1} helium, Honeybee Robotics) that maintains internal pressure requirements during Earth entry and recovery. A diagram of this conceptual sample containment system architecture is given in Figure 14.

After the sample is delivered by the PlanetVac to the singular sample container located in the SRC, the sample transfer valve is closed. Once the last sample attempt is completed, the pneumatic transfer system is separated from the SRC exterior via a tube separation mechanism. Within the SRC, the sample transfer system is also separated from the sample container, and a low leakage rate seal is formed around the sample-side disconnect. The sealing system is TRL 6 technology from the TRL 6 CAESAR New Frontiers comet sample return mission concept (Zacny 2016) and is capable of slowing the rate of sample pressure rise when in Earth atmosphere for the duration of entry/recovery. The aforementioned leak rate means that the internal pressure requirement of $<3 \times 10^{-5}$ Pa is met for an entry/recovery duration of up to 6 hr, assuming the Stardust SRC volume of 0.032 m^3 .

An argon cover gas is used to maintain positive pressure in the volume between the sealed sample container and the outer SRC walls, preventing atmospheric contamination. The cover gas is derived from SRC sample return technology developments (Choukroun et al. 2017).

To prevent aqueous alteration, the sample is actively heated to -20°C early in the return cruise phase to sublime and vent volatiles to space; then, the sample is passively cooled to $<-35^\circ\text{C}$ for the remainder of cruise. Just before Earth entry, the sample venting valve is closed, and both the ammonia

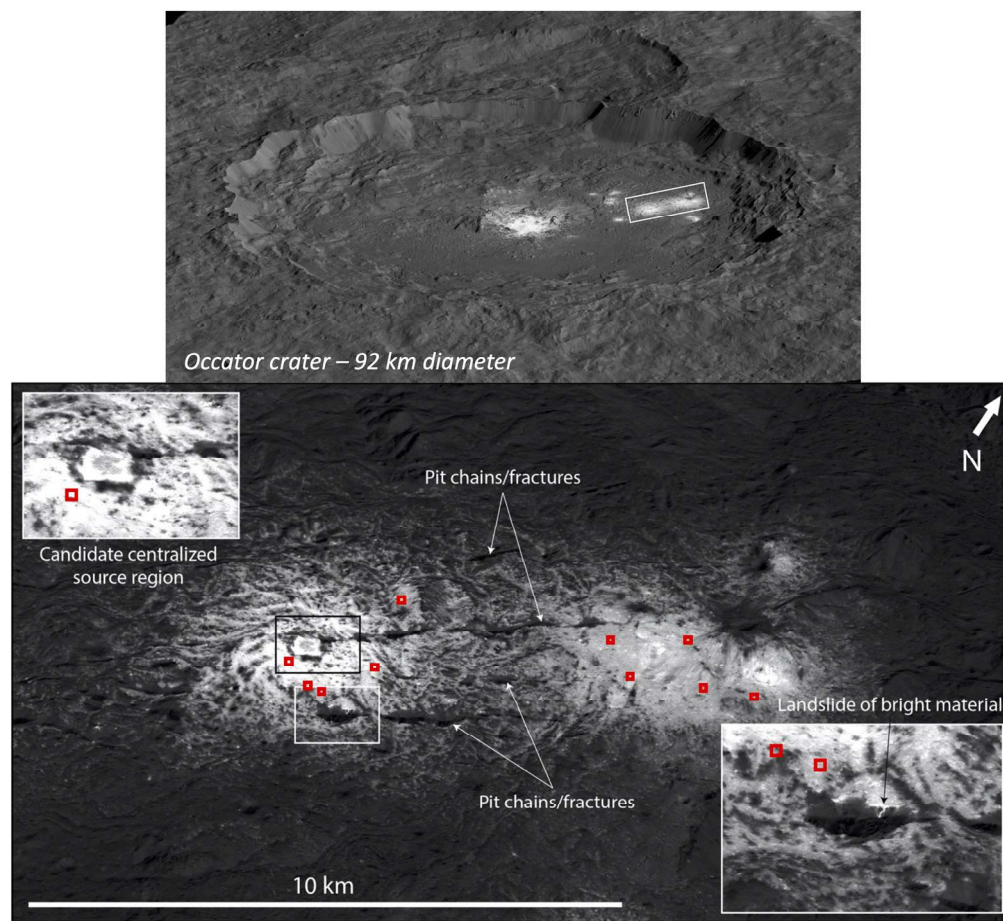


Figure 15. Examples of 100 m diameter safe landing sites, based on Dawn XM2 imaging.

cooling and argon cover gas systems are initiated. The sample is actively cooled and maintained at approximately -35°C , preventing sublimation and aqueous alteration while the sample venting valve is closed during Earth entry/recovery. These systems provide at least 6 hr of both cooling and pressure maintenance of $<3 \times 10^{-5}$ Pa to support recovery operations. The cooling approach is derived from TRL 9 technology from the Orion spacecraft (Lewis et al. 2014; NASA 2015). The sample temperature is measured throughout the journey back to Earth.

The organization for mission implementation (phases A–D) assumes that the spacecraft and SRC are provided by industrial partners under contract to JPL, and separate organizations provide two of the three instruments and the sample acquisition system.

3.3. Concept of Operations and Mission Design

The concept of operations for the sample return mission is divided into seven different phases as described below. The cruise phase is used for both the outbound and inbound heliocentric cruises.

Launch and initial checkout phase. The sample return mission launches from KSC in any year from 2030 through 2037 with little change in overall mission performance. The initial checkout period is expected to be between 30 and 60 days, but no explicit checkout period was included in the trajectory analyses for this study, since that level of detail is not warranted.

Cruise phase. The cruise phase includes both the outbound cruise to Ceres and the inbound cruise back to Earth (Figure 10). The normal state of the vehicle during the cruise phase is thrusting with the IPS. An IPS duty cycle of 90% was assumed in the trajectory analyses. No missed thrust analysis was performed. The SRC is nominally on the shade side of the spacecraft during powered cruise, facilitating its thermal management during the return leg. A summary of mission design parameters, power modes, and communications can be found in Brophy et al. (2022).

Orbital phase. Most of the 500 day stay time at Ceres is in the orbital phase. This phase includes two science orbits, both polar. The 275 km altitude orbit (1:2 resonance) allows the imaging at <3 m pixel^{-1} required to address objectives 1 and 2. Imaging is performed in the visible and two color filters (e.g., 450 ± 20 and 850 ± 20 nm). That phase is accomplished over 90 days. Imaging acquired in this phase is also used to develop a basemap for landing/sampling site selection based on science criteria (from color data) and slopes ($<15^{\circ}$). The current state of understanding based on the Dawn observations indicates that the Vinalia Faculae presents many opportunities for safe landing sites (Scully et al. 2021). Discussion within the science and engineering team, as well as input from the broad community, would lead to the identification of about 10 possible landing areas of about 100 m in diameter based on the slope data and science value. These areas would then be imaged at <30 cm pixel^{-1} from a 28 km altitude orbit for landing/sampling site hazard mapping and certification and to enable precision landing to avoid hazards (i.e., landing within

Table 4
Science Return Comparison for the Two Concepts

Science Objectives	In Situ Homowo Regio Only	In Situ Vinalia Faculae Only	In Situ Homowo and Vinalia	Sample Return Vinalia Faculae
O3. Determine the depth of liquid water below Occator crater.	High science risk; depth of brines in that area is not constrained.	Depth of brine below Vinalia Faculae is constrained to $> \sim 35$ km.		
O4. Characterize Ceres' deep brine environment at Occator crater.	Homowo Regio does not sample current brine reservoir.	Exposed evaporites are evolved from deep brines; composition can be determined with, e.g., Raman spectroscopy, MS, elemental spectroscopy.	Organic matter expected in abundance too small to be detectable with Raman spectroscopy and MS.	Sample return enables full inventory quantification; requires sample to be preserved at $\leq -20^\circ\text{C}$ during return. Trace organic compounds can be fully studied on the ground.
O5. Characterize the evolution of organic matter in long-lived oceans.	Homowo Regio does not sample current brine reservoir.			
O6. Determine Ceres' accretional environment.	<i>Partially addressed with C, H, O, and N isotopes; model-dependent (requires correcting for alteration by hydrothermal processing); light volatile isotopes cannot be uniquely traced to formation in solar nebula, especially as ^{17}O cannot be measured with in situ techniques.</i>	Vinalia Faculae material is likely too processed for origin signature in volatiles to be easily interpreted based on limited analyses with in situ instruments.		Addressed with a variety of measurements, including isotopes of Ti, Cr, Mg, and ^{17}O that are less affected by hydrothermal processing.
Additional objective: constrain the environmental conditions and assess the evolution of organic matter in Ceres' early ocean.	Can be addressed with micro-Raman imaging and isotopes (redox, pH, temperature from clumped isotopes); organic matter expected in high abundance ($\text{[C]} \approx 20$ wt. %), can be characterized assuming compound structure has not been degraded by space weathering (~ 10 Myr timescale); formation conditions of organic compounds with light isotopes (e.g., TLS).	Does not address this objective.		Does not address this objective.
Summary: projected science return.	Obj. 1 and 2 fully addressed; Obj. 6 partially addressed; Obj. 3–5 not addressed; addresses past habitability only	Obj. 1–4 fully addressed; Obj. 5 and 6 not addressed.	Obj. 1–4 fully addressed; Obj. 6 partially addressed; Obj. 5 not addressed.	Obj. 1–6 fully addressed.

Note. This table assesses whether the science objectives are achieved in full (bold text), partially (italic text), or not at all (regular font). An in situ mission and sample return from the Occator evaporites was deemed of greater scientific merit than an in situ mission targeting two sites. Both missions would capture objectives 1–3 in orbit and in situ. The sample return mission concept would be directly responsive to the ROW by quantifying the habitability of Ceres' brines and addressing the fate of organic matter in ocean worlds.

Table 5

The Sample Return Mission Option Provides Better Science at Lower Science Risk and Approximately the Same Development Cost (Phase A–D) as the In Situ Option

Parameter	Sample Return Concept	In Situ Concept
Science		
Science goals	<ol style="list-style-type: none"> 1. Assess Ceres' current habitability and use Ceres as a test case for unraveling the habitability over time of volatile-rich bodies. 2. Determine Ceres' origin and the relationship of its volatiles and organics to other inner solar system bodies. 	<ol style="list-style-type: none"> 1. Assess Ceres' current habitability and use Ceres as a test case for unraveling the habitability over time of volatile-rich bodies. 2. Assess Ceres' past habitability.
Projected science return	<ol style="list-style-type: none"> 1. Progresses along the ROW: <ol style="list-style-type: none"> (i) Assesses extent of material transfer between mantle and surface; (ii) Determines depth of brines below Occator; (iii) Tests whether brines are habitable; (iv) Quantifies extent of prebiotic chemistry. 2. Determines Ceres' origin. 	<ol style="list-style-type: none"> 1. Partially progresses along the ROW: <ol style="list-style-type: none"> (i) Assesses extent of material transfer between mantle and surface; (ii) Determines depth of brines below Occator; (iii) Partially tests whether brines are habitable (does not address prebiotic chemistry) 2. Partially addresses Ceres' origin (association with chondrite only). 3. Partially addresses habitability of Ceres' past ocean (does not address prebiotic chemistry).
Payload	<ol style="list-style-type: none"> 1. Narrow-angle camera 2. Magnetotelluric sounder 3. Point IRS 4. SRC Sampling with PneumaVac system (Honeybee Robotics, HBR)	<ol style="list-style-type: none"> 1. Narrow-angle camera 2. Magnetotelluric sounder 3. Raman imaging spectrometer 4. Tunable laser spectrometer 5. Elemental spectrometer Sampling with PneumaVac system (HBR)
Number of sites	1 (Vinalia Faculae)	2 (Vinalia Faculae and Occator northeastern ejecta), about 40 km apart
Project System		
Launch vehicle	Option 4 (e.g., Falcon Heavy recovery)	
Launch mass	4664 kg	3775 kg
Flight system dry mass (MPV)	2149 kg	2234 kg
Xenon mass	1320 kg	800 kg
Hydrazine mass	1200 kg	701 kg
Cruise time (outbound)	6.5 yr	6.5 yr
Mars gravity assist	Yes	Yes
Orbital phase	Landing site reconnaissance, objectives 1 and 2 for 500 days	
In situ phase	2 months	2 months
Return phase	4.7 yr	N/A
Total phase E duration	12.6 yr	8 yr
Phase F duration	2 yr	6 months after last data acquisition
Planetary protection categorization	V: restricted	II to "IVb-like": depending on landing site (see Castillo-Rogez et al. 2021)

an ~ 20 m diameter area), which is enabled by technologies such as hazard avoidance and terrain-relative navigation (e.g., Johnson et al. 2007). This requirement is consistent with other in situ/sampling missions (e.g., the Europa Lander assumes 50 cm pixel⁻¹; Hand et al. 2017). Texture information obtained at the subpixel level (mottled effect) brings further information on the suitability of the landing site for sampling (Mushkin & Gillespie 2006).

This 5:18 resonant orbit provides 30 flyovers every 1.9 Earth days. This activity requires imaging under five different phase angles for topographic construction based on stereo imaging (one additional angle as margin), for a total duration of 120

days. High-resolution gravity data are also obtained during this phase, and additional imaging and gravity science for opportunistic science may be performed while the final landing site selection and certification activities are proceeding. The time margin for the orbital phase is 4 months. A total data volume of 39 Gbit is returned during the orbital phase.

Deorbit, descent, and landing phase. Deorbit begins from a 28 km orbit altitude with retraction of the solar arrays, followed by a periapsis lowering maneuver. Terrain-relative navigation is used to guide the spacecraft to the preselected landing site. Throttling of the hydrazine propulsion system provides the necessary control. This phase ends with the redeployment of

Table 6
Infrared Point Spectrometer Characteristics

Item	Value	Units
Type of instrument	Point spectrometer	
Number of channels	200 (10 nm spectral resolution)	
Size/dimensions (for each instrument)	0.2 × 0.1 (dia)	m × m
Instrument mass without contingency (CBE ^a)	2	kg
Instrument mass contingency	30	%
Instrument mass with contingency (CBE + reserve)	2.6	kg
Instrument average payload power without contingency	6	W
Instrument average payload power contingency	30	%
Instrument average payload power with contingency	7.8	W
Instrument average science data rate ^b	2.4	kbps
Instrument fields of view	0.2	deg
Pointing requirements (knowledge)	0.05	deg
Pointing requirements (control)	1	deg
Pointing requirements (stability)	0.1	deg s ⁻¹

Notes.

^a CBE = current best estimate.

^b Instrument data rate defined as science data rate prior to onboard processing.

the solar array wings on the surface. Characteristics of the landing area, including an assessment of material properties, are covered by Scully et al. (2021).

Surface phase. The surface phase obtains images of the SEP lander surroundings with the context cameras, including each of the three footpads; operates the point spectrometer as part of addressing objectives 4–6; and deploys and operates the electromagnetic sounder to achieve objective 3. On the surface, the lander will have a mass of about 3400 kg. The surface gravity of Ceres is about 2.8% of Earth's, resulting in a downward force of about 930 N so that no anchoring is needed. The PlanetVac system collects surface samples and stores them in the SRC. Science data from the point spectrometer and electromagnetic sounder are transmitted back to Earth. The total duration of the surface phase is approximately 3 weeks.

Return to Ceres orbit phase. The return to orbit phase begins with retracting the solar arrays. The hydrazine propulsion subsystem provides the thrust to take off from the surface and return to a 28 km orbit altitude. This phase ends with the redeployment of the solar arrays.

SRC Earth entry phase. The Ceres sample return mission uses the UTTR landing site, similar to NASA missions including Stardust, Genesis, and OSIRIS-REx. The U.S. Air Force tracks the SRC from atmospheric entry into the UTTR. After landing, the SRC is recovered, and the samples are delivered to JSC.

Sample curation and analysis phase. Samples are cataloged and curated following the approach described above (see Figure 9). A 2 yr period is dedicated to the analysis of the sample grains necessary to complete objectives 4–6.

3.4. Landing Sites in Vinalia Faculae

In order to identify potential landing/sampling sites, the first priority is spacecraft safety. Using the highest-resolution Dawn data, Scully et al. (2021) found that the majority (>90%) of Vinalia Faculae have slopes of <10°. Scully et al. also identified hazards, such as fractures, pits, and boulders, in Dawn XM2 images (~5 m pixel⁻¹). However, there are numerous smooth patches within the Vinalia Faculae in which no such hazards are visible. Precision landing would be needed to avoid these hazards (i.e., landing within an ~20 m diameter

area), which is enabled by technologies such as hazard avoidance and terrain-relative navigation (e.g., Johnson et al. 2007).

The second priority is the scientifically compelling nature of potential landing/sampling sites. As discussed in Section 1, the Vinalia Faculae region is a highly compelling target because it contains high concentrations of minerals thought to be derived from the deep brine reservoir (Raponi et al. 2019). Moreover, the Vinalia Faculae are made up of relatively thin deposits (no more than ~2–3 m thick, on average) that lie diffusely on top of the dark material that is found throughout Occator crater (Scully et al. 2020 and references therein) with an additional mineral, an aluminum-rich clay, present only in association with the faculae (Raponi et al. 2019). Thus, at Vinalia Faculae, it would be possible to sample both bright facula material and the dark underlying material.

Examples of landing/sampling sites that may be accessible, based on results from the Dawn XM2 (~5 m pixel⁻¹), are shown in Figure 15 and in more detail in Scully et al. (2021). Many more (tens to hundreds) potential 100 m diameter sites exist. Higher-resolution camera (~20 cm to ~1 m pixel⁻¹) and topographic data would be needed to confirm that the slopes in these potential landing/sampling sites are <15° on a lander scale (i.e., on the scale of ~1–5 m), and that hazards are not present at scales smaller than can be resolved in the XM2 data (~5 m pixel⁻¹). Such higher-resolution data would be obtained during the 275 and 28 km altitude orbits discussed above. However, our preliminary analysis indicates that safe and scientifically compelling landing sites do exist in the Vinalia Faculae (see Scully et al. 2021).

3.5. Planetary Protection

A full planetary protection assessment for future missions to Ceres can be found in Castillo-Rogez et al. (2021). The key results from that report relevant to the particular mission concept developed in this paper are summarized here. While necessary for this predecadal study (for costing purposes), this evaluation is not to be considered an official representation position from NASA or the Committee on Space Research (COSPAR).

Table 7
Electromagnetic Sounding Characteristics

Item	Value	Units
Type of instrument	Ceres Magnetotelluric Sounder	
Size/dimensions (for each instrument)	1. 4 × electrodes and launchers (stowed): 22 × 12 (dia) 2. Fluxgate magnetometer and mast (stowed): 12 × 6 × 12 3. Electronics: 15 × 12 × 12	cm × cm
Instrument mass without contingency (CBE ^a)	3.6	kg
Instrument mass contingency	30	%
Instrument mass with contingency (CBE + reserve)	4.7	kg
Instrument average payload power without contingency	6.2	W
Instrument average payload power contingency	30	%
Instrument average payload power with contingency	8.1	W
Instrument average science data rate ^b	5	kbps

Notes.

^a CBE = current best estimate.

^b Instrument data rate defined as science data rate prior to onboard processing.

Table 8
Sample Container Functional Requirements

Sample Container
Hold up to sample mass of 200 g (100 g and 100% margin)
Particulate contamination control to >ISO 5 and nonvolatile organic residue limited to level A/2
Return at ≤−20°C to prevent reaction between anhydrous material and liquid water in the spacecraft
Prevent atmospheric leakage into the SRC during and after Earth entry until SRC recovery
Maintain internal pressure <3 × 10 ^{−5} Pa after SRC closure through SRC recovery

Forward contamination. Forward contamination of the deep brines by spacecraft falling in the large fractures has been evaluated to be a minor concern because the cumulative surface area of these fractures is between 1% and 6% of the surface area of the region targeted by this mission. Based on input from the JPL Biotechnology and Planetary Protection Group, Castillo-Rogez et al. concluded that the outbound leg of this mission (i.e., the lander phase) would likely qualify as “IVb-like” (based on policies developed for Mars rover missions). That is, only the lander equipment in contact with the surface would need to be sterilized, similar to the approach adopted for the Perseverance rover.

Backward contamination. Planetary protection requirements for a sample return mission (Kminek et al. 2017) were assessed, including a quantification of the radiation dosage accumulated by Ceres’ surface material in order to determine whether a sample return mission should be Category V “restricted.” Nordheim et al. (2021) found that sterilization is achieved after about 1 Myr for surficial material down to 10 cm deep. However, considering the large uncertainty on crater-based dating, especially when dealing with salt materials for which little relevant material literature is available, the “restricted” classification is warranted for the sample return missions from the Occator faculae at this time. Hence, a sample return mission would likely be Category V restricted.

We emphasize that this evaluation is preliminary, and the categorization of this concept or derived versions requires

formal assessment by NASA and COSPAR. Furthermore, additional mission design and analysis would assess the risk of, for example, spacecraft failure and access to large fractures.

Pre-Decisional Information—For Planning and Discussion Purposes Only.

The research was carried out at the Jet Propulsion Laboratory, California Institute of Technology, under a contract with the National Aeronautics and Space Administration (80NM0018D0004). © 2021. All rights reserved.

The authors want to thank the following colleagues for their input: Todd White (NASA/ARC); Tom Nordheim, Mohit Melwani Daswani, Mathieu Choukroun, Yang Liu, Yulia Goreva, Brian Clement, James Lambert, Marc Rayman, James Keane, John Mayo, and Christopher Webster (JPL/Caltech); Marc Neveu and Jared Espley (UMD, GSFC); Maria Cristina De Sanctis and Federico Tosi (INAF); Anton Ermakov (UC Berkeley); Christopher Glein, Danielle Wyrick, Ryan Blase, Scot Rafkin, and Mark Libardoni (SwRI); Alien Wang (U. Saint Louis); Karen Meech (U Hawai’i in Manoa); Hajime Yano (ISAS, JAXA); Mikhail Zolotov (ASU); the JPL Formulation Program Office: Kim Reh, James Cutts, Anthony Freeman, Gentry Lee, Howard Eisen, Christophe Sotin, Sabrina Feldman, Gregory Garner, and Rolf Danner; JPL reviewers Samuel Howell, Erin Leonard, and Steve Vance; and external reviewers Erwan Mazarico (GSFC), Vassilissa Vinogradoff (LAM, U. Marseilles), Janet Slate, Colin Dundas, Laszlo Kestay, and Tenielle Gaither (USGS). The authors are also grateful to the following individuals for their contribution to the graphics presented in this manuscript: Allyson Beatrice, Grace Ok, Nicole Sabsook, Corby Waste, Barbara Insua, David Levine, Paul Propster (JPL/Caltech), Raoul Ranoa (raoulranoa.co), Tenielle Gaither (USGS), and Lillian Rose Ostrach.

ORCID iDs

Julie Castillo-Rogez  <https://orcid.org/0000-0003-0400-1038>
 Kelly Miller  <https://orcid.org/0000-0001-5657-137X>
 Michael Sori  <https://orcid.org/0000-0002-6191-2447>
 Jennifer Scully  <https://orcid.org/0000-0001-7139-8050>
 Lynnae Quick  <https://orcid.org/0000-0003-0123-2797>
 Timothy Titus  <https://orcid.org/0000-0003-0700-4875>
 David Williams  <https://orcid.org/0000-0002-7930-9347>

References

- Altair, T., de Avellar, M. G. B., Rodrigues, F., & Galante, D. 2018, *NatSR*, **8**, 260
- Benzerara, K., Menguy, N., Lopez-Garcia, P., et al. 2006, *PNAS*, **103**, 9440
- Bland, M. T., Buczkowski, D. L., Sizemore, H. G., et al. 2019, *NatGe*, **12**, 797
- Brophy, J., Castillo-Rogez, J. C., & Polit Casillas, R. 2022, in *IEEE Aerospace Conf. Proc. (Piscataway, NJ: IEEE)*, 1
- Bouquet, A., Glein, C. R., Wyrick, D., & Waite, J. H. 2017, *ApJL*, **840**, L8
- Bu, C., Rodriguez Lopez, G., Dukes, C. A., et al. 2019, *Icar*, **320**, 136
- Budde, G., Burkhardt, C., & Kleine, T. 2019, *NatAs*, **3**, 736
- Canup, R., & Salmon, J. 2019, *SciA*, **4**, eaar6887
- Castillo-Rogez, J. C. 2020, *NatAs*, **4**, 732
- Castillo-Rogez, J. C., Hesse, M., Formisano, M., et al. 2019, *GeoRL*, **46**, 1963
- Castillo-Rogez, J. C., Neveu, M., McSween, H. Y., et al. 2018, *M&PS*, **53**, 1820
- Castillo-Rogez, J. C., Neveu, M., Scully, J. E. C., et al. 2020, *AsBio*, **20**, 269
- Castillo-Rogez, J. C., Quick, L. C., Neveu, M., et al. 2021, *AsBio*, submitted
- Castillo-Rogez, J. C., & Rayman, M. D. 2020, *NatAs*, **4**, 807
- Chan, Q. H., Stroud, R., Martins, Z., & Yabuta, H. 2020, *SSRv*, **216**, 56
- Chan, Q. H. S., Zolensky, M. E., Kebukawa, Y., et al. 2018, *SciA*, **4**, eaao3521
- Choukroun, M., Mahjou, A., Razzell Hollis, J., et al. 2021, *PSJ*, submitted
- Choukroun, M., Raymond, C., & Wadhwa, M. 2017, *European Planetary Science Congress 2017*, *EPSC2017-413*
- Chyba, C. F. 2000, *Natur*, **403**, 381
- Cockell, C. S., Bush, T., Bryce, C., et al. 2016, *AsBio*, **16**, 89
- Costello, E. S., Ghent, R. R., & Lucey, P. G. 2021, *GeoRL*, **48**, e92960
- De Sanctis, M. C., Ammannito, E., Raponi, E., et al. 2015, *Natur*, **528**, 241
- De Sanctis, M. C., Ammannito, E., McSween, H. Y., et al. 2017, *Sci*, **355**, 719
- De Sanctis, M. C., Ammannito, E., Raponi, A., et al. 2020, *NatAs*, **4**, 786
- De Sanctis, M. C., De Sanctis, M. C., Vinogradoff, V., et al. 2019, *MNRAS*, **482**, 2407
- De Sanctis, M. C., Raponi, A., Ammannito, E., et al. 2016, *Natur*, **536**, 54
- Dworkin, J. P., Adelman, L. A., Ajluni, T., et al. 2018, *SSRv*, **214**, 19
- Ehlmann, B., Blakesberg, J., & Chen, X. 2019, *LPSC*, **50**, 2806
- Ermakov, A. I., Fu, R. R., Castillo-Rogez, J. C., et al. 2017, *JGRE*, **122**, 2267
- Formisano, M., Federico, C., Castillo-Rogez, J., De Sanctis, M. C., & Magni, G. 2020, *MNRAS*, **494**, 5704
- Fu, R., Ermakov, E., Marchi, S., et al. 2017, *E&PSL*, **476**, 153
- Gomes, R., Levison, H. F., Tsiganis, K., & Morbidelli, A. 2005, *Natur*, **435**, 466
- Grimm, R., Castillo-Rogez, J. C., Raymond, C. A., & Poppe, A. 2020, *Icar*, **362**, 114424
- Hand, K. P., Murray, A. E., Garvin, J. B., et al. 2017, *Europa Lander Study 2016 Report JPL D-97667*, <https://europa.nasa.gov/resources/58/europa-lander-study-2016-report/>
- Hendrix, A. R., Hurford, T. A., Barge, L. M., et al. 2019, *AsBio*, **19**, 1
- Hesse, M., & Castillo-Rogez, J. C. 2019, *GeoRL*, **46**, 1213
- Johansen, A., Mac Low, M.-M., Lacerda, P., & Bizzarro, M. 2015, *SciA*, **1**, 1500109
- Johnson, A. E., Ansar, A., Mathies, L., et al. 2007, in *Aerospace 2007 Conf. and Exhibit (Reston, VA: AIAA)*
- Kamata, S., Nimmo, F., Sekine, Y., et al. 2019, *NatGe*, **12**, 407
- Kaplan, H. H., Milliken, R. E., Alexander, C. M., & O'D 2018, *GeoRL*, **45**, 5274
- Kminek, G., Conley, C., Hipkin, V., & Yano, H. 2017, *COSPAR's Planetary Protection Policy*, <https://cosparhq.cnes.fr/assets/uploads/2019/12/PPPpolicyDecember-2017.pdf>
- Koike, M., Nakada, R., Kajitani, I., et al. 2020, *NatCo*, **11**, 1988
- Konopliv, A. S., Park, R. S., Vaughan, A. T., et al. 2018, *Icar*, **299**, 411
- Krujier, T. S., Burkhardt, C., Budde, G., & Kleine, T. 2017, *PNAS*, **114**, 6712
- Le Guillou, C., Bernard, S., Brearley, A. J., & Remusat, L. 2014, *GeCoA*, **131**, 368
- Lewis, J. F., Barido, R. A., Boehm, P., Cross, C. D., & Rains, G. E. 2014, 44th Int. Conf. on Environmental Systems, ICES-2014-038
- Li, L., Cartigny, P., & Ader, M. 2009, *GeCoA*, **73**, 6282
- Li, L., Sherwood Lollar, B., Li, H., Wortmann, U. G., & Lacrampe-Couloume, G. 2012, *GeCoA*, **84**, 280
- Marchi, S., Raponi, A., Prettyman, T., et al. 2019, *NatAs*, **3**, 140
- McCubbin, F. M., Herd, C. D. K., Yada, T., et al. 2019, *SSRv*, **215**, 48
- McSween, H. Y., Emery, J. P., Rivkin, A. S., et al. 2018, *M&PS*, **53**, 1793
- Meech, K. J., & Raymond, S. N. 2020, in *Planetary Astrobiology (Space Science Series)*, ed. V. Meadows et al. (Tucson, AZ: Univ. Arizona Press), 32
- Melwani Daswani, M., Vance, S. D., Mayne, M. J., & Glein, C. R. 2021, *GeoRL*, **48**, e94143
- Milam, S., Dworkin, J. P., Elsila, J. E., et al. 2021, *BAAS*, **53**, 049
- Mushkin, A., & Gillespie, A. R. 2006, *GeoRL*, **33**, L18204
- NASA 2015, *Technology Roadmap, TA 14: Thermal Management Systems*, https://www.nasa.gov/sites/default/files/atoms/files/2015_nasa_technology_roadmaps_ta_14_thermal_management_final.pdf
- NASEM 2019, *Strategic Investments in Instrumentation and Facilities for Extraterrestrial Sample Curation and Analysis* (Washington, DC: The National Academies Press)
- NASEM 2020, *Planetary Science and Astrobiology Decadal Survey 2023–2032*, https://sites.nationalacademies.org/SSB/ssb_198172
- Nathues, A., Schmedemann, N., Thangjam, G., et al. 2020, *NatAs*, **4**, 794
- Neveu, M., & Desch, S. J. 2015, *GeoRL*, **42**, 10,197
- Neveu, Marc, Desch, Steven J., & Castillo-Rogez, Julie C. 2017, *GeCoA*, **212**, 324
- Nordheim, T., Castillo-Rogez, J. C., Villarreal, M., Scully, J. E. R., & Costello, E. 2021, *AsBio*, in press
- Park, R. S., Konopliv, A. S., Ermakov, A. I., et al. 2020, *NatAs*, **4**, 748
- Pieters, C. M., Nathues, A., Thangjam, G., et al. 2018, *M&PS*, **53**, 1983
- Prettyman, T. H., Yamashita, N., Ammannito, E., et al. 2018, *Icar*, **318**, 42
- Prettyman, T. H., Yamashita, N., Toplis, M. J., et al. 2017, *Sci*, **355**, 55
- Quick, L., Buczkowski, D. L., Ruesch, O., et al. 2019, *Icar*, **320**, 119
- Raponi, A., De Sanctis, M. C., Frigeri, A., et al. 2018, *SciA*, **4**, eaao3757
- Raponi, M. C., De Sanctis, F. G., Carrozzo, M., et al. 2019, *Icar*, **320**, 83
- Raymond, C. A., Ermakov, A. I., Castillo-Rogez, J. C., et al. 2020, *NatAs*, **4**, 741
- Raymond, S. N., & Izidoro, A. 2017, *Icar*, **297**, 134
- Ruesch, O., Genova, A., Neumann, W., et al. 2019a, *NatGe*, **12**, 505
- Ruesch, O., Platz, T., Schenk, P., et al. 2016, *Sci*, **353**, aaf4286
- Ruesch, O., Quick, L. C., Landis, M. E., et al. 2019b, *Icar*, **320**, 39
- Scully, J. C., Baker, S., Castillo-Rogez, J. C., & Buczkowski, D. L. 2021, *PSJ*, **2**, 94
- Scully, J. E. C., Schenk, P. M., Buczkowski, D. L., et al. 2020, *NatCo*, **11**, 3680
- Sori, M. M., Byrne, S., Band, M. T., et al. 2017, *GeoRL*, **44**, 1243
- Sori, M. M., Sizemore, H. G., Byrne, S., et al. 2018, *NatAs*, **2**, 946
- Tsou, P., Brownlee, D. E., McKay, C. P., et al. 2012, *AsBio*, **12**, 730
- Turner, N. J., Choukroun, M., Castillo-Rogez, J. C., & Bryden, G. 2012, *ApJ*, **748**, 92
- Vance, S. D., Hand, K. P., & Pappalardo, R. T. 2016, *GeoRL*, **43**, 4871
- Vernazza, P., Castillo-Rogez, J., Beck, P., et al. 2017, *AJ*, **153**, 72
- Vinogradoff, V., Bernard, S., Le Guillou, C., & Remusat, L. 2018, *Icar*, **305**, 358
- Vinogradoff, V., Le Guillou, C., Bernard, S., et al. 2017, *GeCoA*, **212**, 234
- Warren, P. H. 2011, *E&PSL*, **311**, 93
- Walsh, K. J., Morbidelli, A., Raymond, S. N., O'Brien, D. P., & Mandell, A. M. 2012, *M&PS*, **47**, 1941
- Willacy, K., & Woods, P. M. 2009, *ApJ*, **703**, 479
- Zacny, K. L. 2016, *Development of a Hermetically Sealed Canister for Sample Return Missions SBIR/STTR*, 154580
- Zacny, K., Lorenz, R., Rehnmark, F., et al. 2019, in *2019 IEEE Aerospace Conf. (Piscataway, NJ: IEEE)*, 1
- Zacny, K. L., Thomas, G., Paulsen, D., et al. 2020, in *2020 IEEE Aerospace Conf. (Piscataway, NJ: IEEE)*, 1
- Zolensky, M. E., Bodnar, R. J., Yurimoto, H., et al. 2017, *RSPTA*, **375**, 20150386
- Zolotov, M. Y. 2020, *Icar*, **335**, 113404